WAVE DIRECTIONALITY IN PERIODIC LATTICE STRUCTURES

A Thesis by

Sreeram Saran Vanam

Bachelor of Technology, JNTU, Hyderabad, Telangana, 2016

Submitted to the Department of Aerospace Engineering
and the faculty of the Graduate School of
Wichita State University
in partial fulfillment of
the requirements for the degree of
Master of Science

December 2019

WAVE DIRECTIONALITY IN PERIODIC LATTICE STRUCTURES

The following faculty members have examined the final copy of this thesis for form and content and recommend that it be accepted in partial fulfillment of the requirement for the degree of Master of Science with a major in Aerospace Engineering.

Bhisham N. Sharma, Committee Chair

Charles Yang, Committee Member

Bukhgeym, Alexander, Committee Member

DEDICATION

To my parents, Hemalatha and Yogananda Rao Vanam

ACKNOWLEDGMENTS

I want to express my sincere gratitude to my advisor Dr. Bhisham Sharma for continued guidance and support. The endless patience and knowledge you gave me shaped me as a person, helped me develop my skills into regions I could never have imagined at the start of my degree. It has been a privilege to work with him and to gain knowledge in the field of vibrations and structural dynamics.

Secondly, I thank my committee members, Dr. Charles Yang and Dr. Bukhgeym Alexander, for their time and valuable suggestions. Thank you for all your valuable comments. I would also like to extend my deepest gratitude to my friends and family for their constant support and backing me during hard times.

I want to thank all the members of Mechanics and Dynamics Lab. I learned a lot from each one of you and had fun inside and outside the lab.

ABSTRACT

We discuss the wave directionality for in-plane and out-of-plane waves in three-dimensional self-similar and non-self-similar square periodic lattices. The lattices studied are square lattice, square in the square hierarchical lattice, and hexagon in a square hierarchical lattice. Finite Element Analysis is used to calculate dispersion relations and directionality properties for these lattice structures following a 25/25 grid covering the complete Brillouin zone. The investigation is performed by combining the Floquet-Bloch theory of periodic structures with the commercial FE solver, Comsol Multiphysics. A method to distinguish between the in-plane and out-of-plane wave modes is explained in detail. Multiple surfaces are selected to show that the dispersion surfaces overlap in frequency and beaming direction; thus, requiring an efficient way to distinguish the in-plane and out-of-plane modes. The effects of the hierarchy on the wave beaming in the chosen lattices are studied. The in-plane waves are observed to beam mostly along 0° and 90° directions in the square lattice, while a more equal spread is observed for the hierarchical lattices. Significant beaming is observed in the hexagon in the square lattice for the out-of-plane waves. The effect of hierarchy on the generation of bandgaps is studied. Compared with a non-hierarchical square lattice, the hierarchical lattice structures display significantly lowered group velocity magnitudes. The non-self-similar hierarchical lattice was found to provide bandgaps at lower frequencies and slower group velocities as compared to the self-similar hierarchical lattice.

TABLE OF CONTENTS

TABLE OF CONTENTS (continued)

Chapter Page

LIST OF TABLES

LIST OF FIGURES

LIST OF FIGURES (continued)

Figure Page

Figure Page

NOMENCLATURE

L	The edge length of zero-order hierarchical lattice
L_y	Length of the unit cell in the y-direction
L_x	Length of the unit cell in the x-direction
u	Displacements in the x-direction
v	Displacements in the y-direction
u^*	Unit vector
w	Displacements in the z-direction
t^*	time
t	thickness
h	Thickness in z-direction
λ	Wavelength
k	Wavenumber
k	Wave vector
k_1, k_x	Wave vectors in the x-direction
k_2, k_y	Wave vectors in the y-direction
c	Wave speed
c_0	Longitudinal wave speed
∅	Direction of wave propagation
φ	Phase
v_p, V_p	Phase velocity
v_g, V_g	Group velocity
ϟ	Magnitude of the group velocity
ω	Frequency of Plane Wave
q_u	Forcing function
M, M^{gq}	Mass matrix
K	Stiffness Matrix
$\ddot{\mathbf{U}}$	Acceleration Vector

U	Displacement vector.
F	Force vector
ψ	Eigenvector matrix
r	Edge side length or radius of first order hierarchy
Υ	Characteristic length ratio
β	in-plane ratio
ρ_0	Relative density
ρ_c	The ratio of the density of the cellular structure
ρ_s	The density of the whole solid
ϑ	Poisson's ratio
E	Young's modulus
I	The second moment of inertia
D	Plate flexural rigidity
∇	Differential operator
ρ	Density
$\acute{\omega}$	Normalized frequency
ω_0	Frequency of the given boundary condition
α	Eigenmode
m_α	Generalized mass of the structure
$P_{\alpha i}$	Participation factor
P_1, P_2 & P_3	participation factors in the directions x, y, & z.
T_i	Influence matrix
P	Waves traveling along the direction of vibration
S	Waves do not travel along the direction of vibration
Γ, X, M, Y, Y', X', M'	High symmetry points
IBZ	Irreducible Brillouin zone
FBZ	First Brillouin zone

1. INTRODUCTION

1.1 Periodic structures

A periodic structure is a finite or infinite repetition of a unit cell in one, two, or three dimensions [1]. Periodic structures have a long history in the field of vibrations and acoustics, starting from Newton's first attempt to describe the propagation of sound in the air [2] and Rayleigh's studies on the dynamic behavior of the continuous periodic structures [3]. Over the past decades, the dynamic behavior of continuous structures have been extensively, particularly with a view towards acoustic and vibration mitigation applications [4, 5], Recently, the focus has shifted to periodic materials or structures, also known as phononic materials. A phononic medium is a material/system that exhibits some form of periodicity either in the material composition, internal geometry, or the boundary conditions.

According to Ref. [6], the attempt to derive the formula for the sound in air by Newton resulted in the first work on a one-dimensional 1D periodic beam lattice. Figure 1. Shows a periodic system with a series of lumped masses connected by a lumped spring. This system has a more complex wave behavior than a typical continuous system.

[6]John Bernoulli and his son Daniel Bernoulli first studied this system and demonstrated that n natural vibration modes characterize a system of N masses. Subsequent studies included the estimation of the wave propagation velocity as a function of the wavelength along one axis of a cubic lattice structure. These efforts lead to the study of wave dispersion from the estimations of the phase velocity's dependency on the frequency.

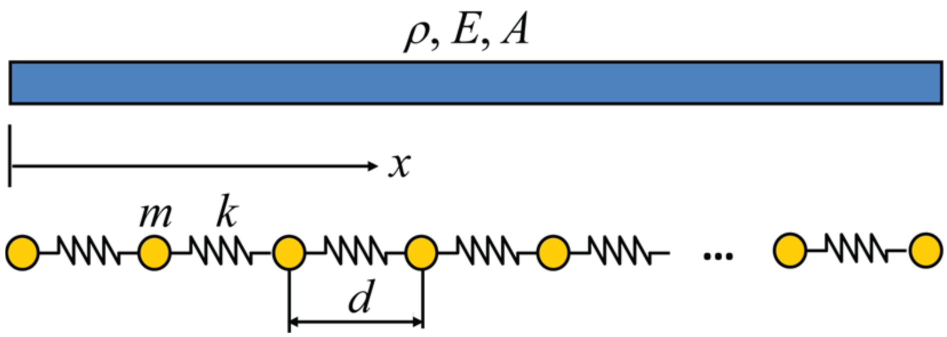

Figure 1. Discretization of a rod into spring-mass lattice [7]

Since those early days, numerous researchers in vibrations, acoustics, and mechanics have studied the dynamic behavior of periodic systems such as composite materials [8, 9], and aircraft structures—which naturally exhibit some degree of periodicity due to the presence of ribs introduced primarily for strengthening and stiffening purposes [10, 11]. Other examples include multi-blade turbines [12-14], impact-resistant cellular foams [15-17], periodic foundations and reinforcements for buildings [18, 19] and multistory buildings [20].

Figure 2. Beehives created by honeybees display a periodic honeycomb structure.

A good example of periodic structure in nature is a beehive created by honey bees displaying a periodic honeycomb structure. A beehive with periodic nature in x and y directions is shown in Figure 2. There are human-made or artificial periodic structures. One of the best examples of the artificial periodic structure is a simple railway track [21]. It is the best example of a periodic structure in a single direction as shown in Figure 3. The designs used in this work are other examples of artificial periodic structures. For instance, a simple square unit cell and its periodic form are shown in Figure 4

Figure 3. Railway track indicating a periodic structure in a single direction.

.

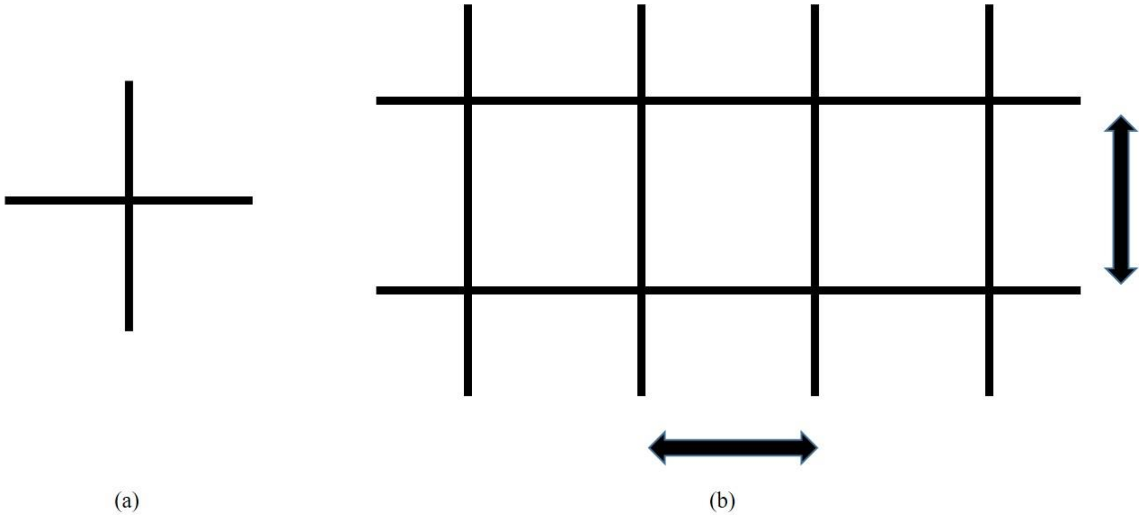

Figure 4. (a) Square unit cell, (b) Infinite periodic structure of the square unit cell (arrows indicating periodicity in x and y directions).

Elastic wave propagation in phononic crystals is governed by the Floquet-Bloch theorem [6], which allows the calculation of the dispersion curves of an infinite periodic structure by analyzing only a repeating unit cell within its Irreducible Brillouin Zone (IBZ) [4]. Phononic materials exhibit wave attenuation bandgaps, i.e., frequency intervals within which wave propagation through the material is prohibited [7, 22]. These bandgaps are created due to the impedance mismatch due to discontinuities in geometry or material within the structure which results in destructive wave interference at specific frequencies [23]. These bandgaps can be altered in many ways based upon the lattice topology and material properties. Further bandgaps may be generated by including locally resonant subsystems, changing the geometric parameters like lattice skewness, the order of hierarchy, void volume fraction, and various other mechanical properties.

There are different kinds of bandgaps, such as directional bandgaps, polarized bandgaps, and complete bandgaps. In general, we confine the set of wave vectors to be investigated to the first Brillouin zone defined in the reciprocal lattice space [24], which lies in the same surface plane as the direct lattice [25]. Exploiting the symmetry of the structure further reduces the set of wave vectors to be analyzed to the irreducible Brillouin zone [26]. Bandgaps occurring along particular wave propagation directions are called directional bandgaps. In general, elastic waves can be classified as P-polarized or S-polarized waves [27]. P-waves are waves that exhibit particle motion parallel to the wave propagation direction, while propagation modes with non-parallel particle motions are classified as S-waves. The classification can be made by using modal participation factors. A complete bandgap indicates the restriction of the wave propagation in all the directions in a structure.

The location and width of stopbands are dependent on the direction of the wave propagation with respect to the structure's geometry [28]. Phononic crystals are also shown to have frequency-dependent wave beaming/steering characteristics with applications in wave attenuation and guiding [22-24]. Wave beaming is simply the directional energy flow in a structure. Structures are typically designed with an idea of increasing the stability, efficiency, and various other properties to ultimately increase the life of the structure with increased advantages of it in different ways possible. Understanding the directional behavior of a structure helps better understand the vibrational characteristics of the structure and thus improve its dynamic properties. The understanding can also be used to tailor the wave propagation characteristics of the structure.

Wave directionality of lattices occurs due to partial wave filtering along with specific spatial directions, which forces the waves to propagate in the remaining angular directions. Several techniques have been developed to represent beam/steering or directionality characteristics of periodic lattices. Among them are constant-frequency contour plots, phase continuous surfaces, phase, and group velocity plots, polar group velocity contours [23, 29]. The group velocity polar contour plots are a good representation of the isotropy/anisotropy in the elastic medium along the plane of wave propagation and predict the direction of wave propagation at specific frequencies. The evaluation of group and phase velocities allows determining the dispersive behavior of the lattice, highlighted by the frequency dependence of the phase velocity, and the anisotropy of the domain in the wave propagation plane. By evaluating the group velocity polar plots, we can tell about the directivity with ease, which helps in predicting the regions where the energy cannot flow, which later is useful in tailoring the structure according to our needs.

From the iso-frequency contour plots, we can derive the phase and the group velocity plots, which are good sources in determining the directionality. Phase velocity is defined as the speed at which the wave is traveling in terms of the frequency corresponding to the wave vector. The dispersion relation provides the relationship between the frequency and the wave vector. The slope of the secant to the dispersion curve at any frequency gives the phase velocity at that frequency [30]. In a medium without any damping or dispersion, the phase velocity plots are circular with a constant radius independent of frequency. A circular plot means the waves are propagating in all directions. Group velocity is defined as the energy flow associated with the propagation of the wave packets within the lattice structure. For a given frequency, the direction of the energy flow within the structure is identified by the normal to the iso-frequency plots, or it can be represented more accurately through a polar group velocity plot.

1.2 Literature review

Extensive efforts have been made to analyze the wave propagation in periodic structures, which comprise of a few identical components combined in an identical manner. Rayleigh's studies on string vibrations [31] and Brillouin's analysis on lattice vibrations [6] provide the initial foundational basis on the analysis of wave motion in periodic systems. Starting with spring-mass configurations [6] and one-dimensional beams [32], there are numerous methods to study the wave motion in periodic structures. Mead [11, 33-35] provided receptance methods to find the dispersion behavior of structures. Other researchers have developed methods including direct solutions of differential equations of motion [34], transfer matrix methods [36, 37], energy methods [38, 39], and space-harmonic analysis [40] to further understand the wave motion characteristics of periodic structures.

Recent research efforts have focused on studying wave propagation in discrete geometries to control the dispersion characteristics and obtain tunable wave attenuation and waveguiding properties. Periodic lattice materials have gained more attention due to recent advances in additive manufacturing techniques and the resultant ability to control their geometrical and material properties. Researches have studied lattice truss structures with high stiffness and strength [41], mechanically superior cellular solids [42, 43], and cellular materials with improved energy absorption [44]. Structural lattices also admit elastic stress wave control and continue to be of topical interest for waveguiding [7].

Bayat and Gaitanaros [45] focused on elastic wave propagation in three-dimensional (3D) low-density lattices and explored their wave directionality and energy flow characteristics. In particular, they examined the dynamic response of Kelvin foam, simple cubic, framed cubic, and octet truss lattices using iso-frequency contour plots. Using four-dimensional velocity plots to represent the directionality, they demonstrated that the framed cubic lattices provide wider bandgaps than other structures. Foehr et al.[46] studied wave beaming in spiral-based phononic plates and demonstrated their use as topological insulators. Using iso-frequency contour plots, they found showed the unit cell symmetry can be modified to increase the number of bandgaps due to simultaneous Bragg scattering, local resonance, and inertial amplification effects. Vibration characteristics of metamaterial plates manufactured from assemblies of periodic cells with built-in local resonators are presented in [47]. In this work, the directivity plots are used to indicate that metamaterial plates are more effective in attenuating and filtering low-frequency structural vibrations than plain periodic plates of similar weight and size.

The existence of “retro-propagating” Bloch wave modes with a negative group velocity and the corresponding retro-propagating frequency bands are highlighted in [48]. In this, the phase and group velocities of the Bloch eigenmodes are calculated to analyze the anisotropic behavior of the hexagonal lattice structure. Wave motion is prevented between certain frequency ranges, generating bandgaps in specific directions as a result of undulation-induced anisotropy in [48]. In this, the phase and group velocities of the Bloch Eigenmodes are calculated to analyze the anisotropic behavior of the hexagonal lattice structure. Wave motions are prevented under specific frequency ranges, generating bandgaps in specific directions as a result of undulation-induced anisotropy in [29].

Wave propagation in auxetic star-shaped honeycombs is investigated in [49]. The authors study the effects of different kinds of polymer fillings on the dispersion behavior using iso-frequency contour plots and conclude that among three filling types, the outer-filled honeycomb has the best collimation effect. Variation of the dispersion, bandgap occurrence, and the wave directionality is investigated in[50]. Bacigalupo and Lepidi [27] studied the energy transport-related to dispersive waves propagating through non-dissipative micro-structured materials. Wang et al. [51]. Studied the directional propagation of elastic waves in two-dimensional zig-zag lattice structures. They compare the iso-frequency curves with polar plots of the directional wave propagation to study the effects of energy propagation along the lattice arms to understand the concentricity of the directional wave propagation. Wave directionality related to the effective anisotropic mechanical properties is discussed in [52]. Directionality plots are derived for the associated frequencies to study the dynamic response of a tunable phonic crystal under applied mechanical and magnetic loading in [53]. It is shown that magnetic induction not only controls the band diagram but also has a strong effect on the preferential directions of the wave propagation of the structure.

A traditional way to evaluate the direction of the gradient is to use iso-frequency contour plots of the dispersion surfaces [54]. Using the iso-contour plots became common until [23] has analyzed the direction of wave propagation in a regular hexagonal grid using polar plots to represent the directionality of the wave propagation. This is achieved by fitting continuous functions to the iso-frequency contours, which allows us to calculate the direction of the group velocity by differentiation. Zelhofer and Kochmann [55] have recently introduced a new methodology to analyze the directional group velocity distributions.

1.3 Objective

The objective of this research is to study the wave directionality effects in self-similar and non-self-similar hierarchical lattice structures. Our primary focus is to develop a new method that leverages polar plots to represent the wave directionality in periodic structures better. Here, we apply the developed method to study the directionality of three different structures: (1) a square lattice structure, (2) a self-similar square in a square hierarchical lattice structure, and (3) a non-self-similar hexagon in a square lattice structure. Though significant work has recently been done to study the directional behavior of 2D and 3D lattice structures, little attention has been paid to the effects of hierarchy on directionality.

Our objective is to adapt the group velocity polar plot methodology proposed by Zelhofer and Kochmann [55] to isolate the in-plane and out-of-plane wave modes and study the effect of lattice topology on their directionality. The focus is on moving beyond traditional iso-frequency contour plots and using polar plots derived by fitting continuous functions to the iso-frequency contours instead. Our intent is to use a commercial FE software to obtain the dispersion surfaces of the chosen periodic structures and use them to generate continuous group velocity maps that show the relative wave velocity magnitudes and direction. The developed method will help better analyze wave beaming in periodic structures in the future and provide engineers with better control over the dynamic behavior of such structures.

Thesis outline

In the following chapters, improved concepts to describe and predict the group velocity magnitude and direction are shown. Chapter 2 reviews the fundamentals of wave propagation in engineering structures. A summary of wave directionality is provided. Chapter 3 focuses on the methodology of deriving dispersion surfaces and extracting the in-plane and out of the plane surfaces using modal participation factors. Details about the unit cells and their geometrical properties used in this research are provided. Chapter 4 shows the results obtained for the directional wave propagation. Beaming predictions are compared between the lattice structures, and the generation and extension of bandgaps and the partial bandgaps are explained for each structure in detail. Out-of-plane dispersion surfaces and velocity plots are shown for all the structures. Finally, Chapter 5 concludes this thesis and summarizes potential future work.

2. WAVE PROPAGATION IN ENGINEERING STRUCTURES

2.1 Short introduction to wave propagation:

Wave propagation means waves traveling inside a structure. Energy propagates inside the structure in the form of waves in space and in time. The disturbance caused inside a structure transfers energy through medium or space with no mass transfer is called a wave. There are two types of wave motions: longitudinal and transverse waves as shown in Figure 5. In longitudinal waves, the direction of the wave propagation is parallel to the particle displacement. In transverse waves, the direction of the wave propagation is perpendicular to the particle displacement [56]. Waves in large structures do not interact with the boundaries resulting in space/time relation for the location of the energy. Waves in small structures cause excessive wave reflections resulting in vibration characteristics [2].

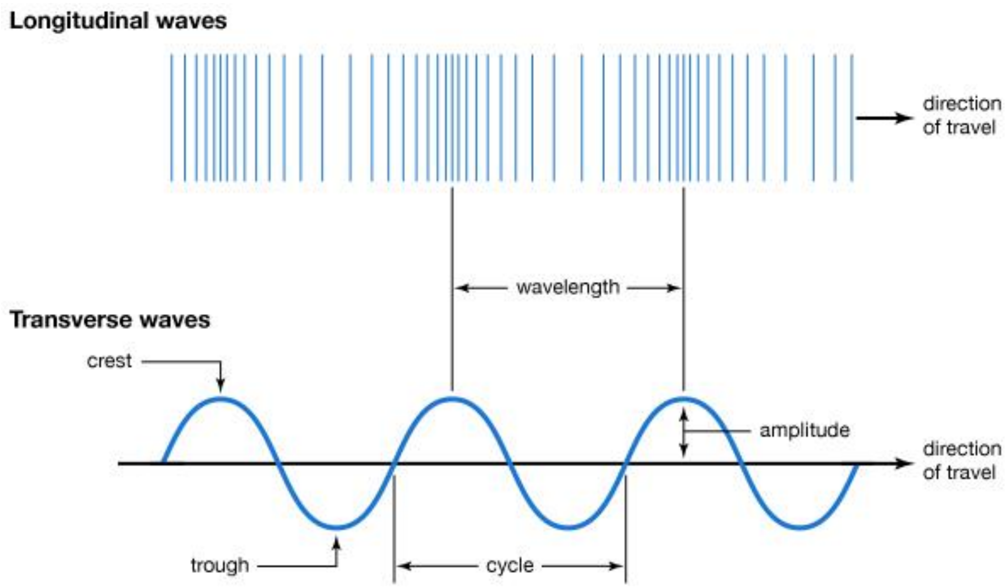

Figure 5. Longitudinal and transverse waves [57]

During wave propagation, the structure excites at various frequencies. The effective modal mass provides a method for predicting the direction of the wave propagation of modes. The equation which governs the discrete dynamic system is

$$\mathbf{M\ddot{U} + KU = F} \tag{1}$$

Where M is the mass matrix and K is the stiffness matrix

Ü Is the acceleration vector, U is the displacement vector, and F is the force vector.

Taking the direction of wave modes into consideration, waves are again classified as a P wave and an S wave. If the vibration of the structure and the wave propagation in the structure are in the same direction, then it is said to be P wave, and they are in different directions for an S wave. In general, participation factors are used to differentiate these.

Waves can propagate in different types of media. Some examples are Rayleigh surface waves, elastic waves, and acoustic waves. The elastic wave equation describes the propagation of elastic disturbances produced by seismic events in the earth or vibrations in plates and beams [58]. The acoustic wave equation governs the propagation of sound. Waves also propagate in slender members with traction-free lateral boundary conditions such as rods, and beams [2]. Slender members are also known as waveguides. Our study here is confined to the slender members ignoring the other types of extended media. The spectral analysis approach is considered to study these slender members.

Any arbitrary time signal can be achieved from the super-position of many sinusoidal components, i.e., it has a spectrum of frequency components. Working in terms of the spectral components is called ‘spectral analyses or ‘frequency domain analysis.’ The spectral analysis gives away all the physical information about the waves. The general equation of the wave is derived by using spectral analysis and spectral relations.

$$u(x, t^*) = \sum C_1 . e^{i(\mathbf{k}x - \omega t^*)} + \sum C_1 . e^{-i(\mathbf{k}x - \omega t^*)} \tag{2}$$

Where, $\varphi = (\boldsymbol{k}x - \omega t^*)$ is called the phase of the wave, and ω is the angular frequency and C_1, C_2 are known as the amplitude spectrum and are the functions of frequency. ‘**k**’ is called the wavenumber.

Wavenumber is also known as the spatial frequency and is defined as the number of cycles per unit length. It is the scaling for the spatial variable in the spatial domain. The relation between wavenumber, **k**, and frequency, ω is called the “spectrum relation.” The vector indicating the direction of wave propagation and perpendicular to the wavefront is called the wave vector.

Wavenumber is the magnitude of the wave vector, and it is defined as $k = \frac{2.\pi}{\lambda}$, where λ is the wavelength. They are clearly mentioned in Figure 6.

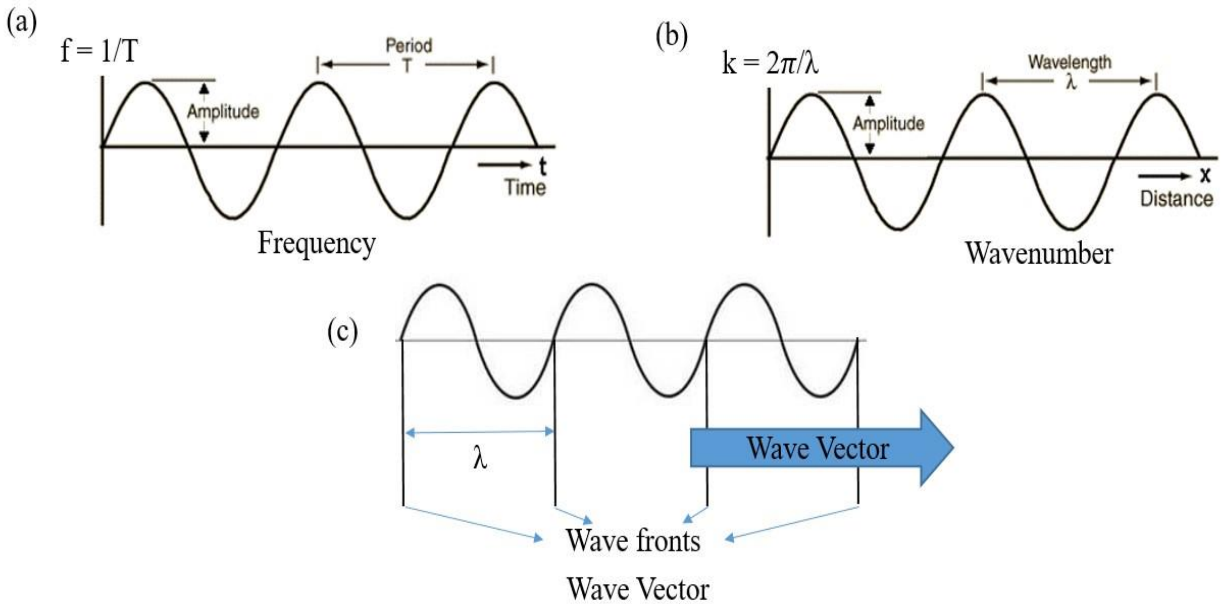

Figure 6. (a) Frequency (b) Spatial frequency or wavenumber (c) Wave vector [59]

2.2 Idea of dispersion through the wave behavior in rods, beams, and plates

Apart from the fact that the waves are of different types, waves are dispersive and non-dispersive. As discussed before, they propagate in slender members like rods, and beams as well as plates.

In rods, the displacements are assumed to be axial, and the Poisson's ratio is neglected. When a rod is hit, the load applied compresses it locally, and when the load is removed, it gets back to the normal stage. These kinds of waves are called the compressive/tensile/pressure longitudinal waves.

The basic equation of motion of slender rod with uniform properties is

$$EA\frac{\partial^2 u}{\partial x^2} = \rho A\frac{\partial^2 u}{\partial t^2} + q_u(x,t) \tag{3}$$

Where the damping and the Poisson's ratio are neglected. In Equation.3, $q_u(x,t)$ is the forcing function, E is Young's modulus, ρ is the density of the material used, and I is the moment of inertia. This equation is called the "wave equation."

In beams, the waves are flexural. They can support transverse loads through flexure. The primary assumption that is considered in the case of beams is that when a force is applied, the motion is in the transverse direction, and the cross-sections can rotate but remain plane [2].

The equation of motion for a beam is

$$EI\frac{\partial^4 v}{\partial x^4} + \rho A\frac{\partial^2 v}{\partial t^2} = q_v(x,t) \tag{4}$$

Plate components are three-dimensional. They are relatively thin along specific axes which is why they are represented as two-dimensional elements. They can exhibit flexural rigidity about their local axes. Thickness is the only reduced dimension of a plate [60]. Especially under the plane stress conditions, though plates are three dimensional, their behavior is two dimensional.

The governing equation of the plate is

$$\mathrm{D}\nabla^2\nabla^2 w + \rho h\frac{\partial^2 w}{\partial t^2} = q_w \tag{5}$$

Where w is the transverse deflection and h is the thickness in the z-direction, and

$$\nabla = \frac{\partial^2}{\partial x^2} + \frac{\partial^2}{\partial y^2} \tag{6}$$

$$D = \frac{Eh^3}{12(1-\vartheta^2)} \tag{7}$$

2.2.1 Dispersion

The phase is an essential factor in a wave that describes the location of a point in the wave at a particular moment. In spectral analysis, the work done is in the frequency domain. We know that the wavenumber is also referred to as the spatial frequency. The equation of phase as before is $\varphi = (\boldsymbol{k}x - \omega t)$. From this, phase speed is written as $v_p = \frac{\omega}{k}$, which represents the relation between c_p and ω. This relation between the phase speed and frequency is known as the "dispersion relation." Also, the relation between the wavenumber, **k**, and the frequency, ω is called the "spectral relation." These relations have many points that relate the wave vector and the frequency, which when combines to result in the "dispersion curves."

If the phase speed of the wave is constant with respect to the frequency, then the wave is non-dispersive. From the spectral analysis of wave motions, the wavenumber '**k**' for a rod, and beam are

Table 1. Wave number equations for a rod and beam.

Member	**Wavenumber, k**
Rod	$\boldsymbol{k}(\omega) = \omega \left(\frac{\rho A}{EA}\right)^{\frac{1}{2}} = \frac{\omega}{c}$
Beam	$\boldsymbol{k}(\omega) = \sqrt{\omega} \left(\frac{\rho A}{EI}\right)^{\frac{1}{4}} = \sqrt{\frac{\omega}{c_0 h}} 12^{\frac{1}{4}}$

From Table 1., the relation $\boldsymbol{k}(\omega)$ is the spectrum relation and is plotted for the rod and beam.

In general, the plot representing the spectral relation shows the variation of the **k** concerning the frequency. Figure. 7 displays a curve relating to the wavenumber and the frequency.

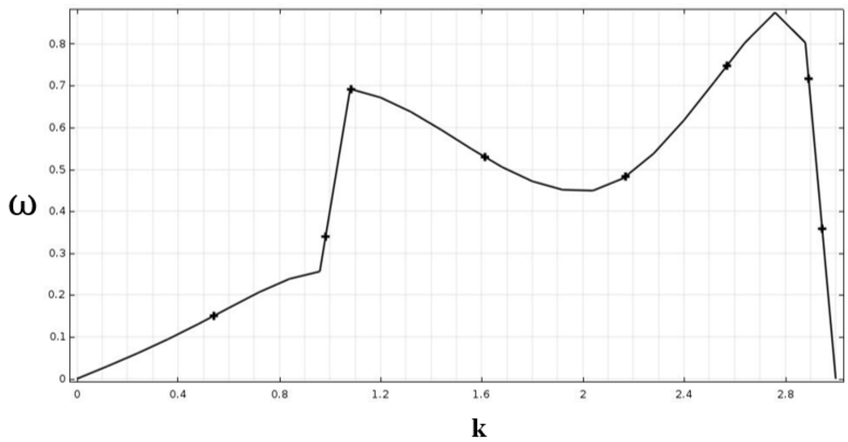

Figure 7. Dispersion curve

Where the line in Figure 7. is called a dispersion curve.

2.2.2 Wave velocity:

The distance traveled by a periodic motion or cyclic motion per unit time is known as the wave velocity [57]. According to Leon Brillouin [6], the velocity of the waves is defined as giving the phase difference between the vibrations observed at two different points in a free plane wave. It gives information about the magnitude of the wave and the direction in which the wave is traveling. In general, the velocity of a wave is equal to the product of its wavelength and frequency [57]. From a physics point of view, this wave velocity is divided into two different types of velocities which might be equal in some situations. They are the phase velocity and group velocity. Both of them describe the wave characteristics across the media.

Phase velocity is defined as the speed at which the wave is traveling in terms of the frequency corresponding to the wave vector (in the direction of **k**). It is the same as the phase speed. It majorly speaks about the speed at which the particles are jiggling inside a wave. In general, we can look at a wave motion at a particular moment. Compare its position at some point at a different time. Any observations related to the change of positions of the wave forward or backward from its original position would tell us about the phase velocity or the phase speed. In simple terms, we need to look at how fast the shape is traveling/moving.

Phase velocity is formulated as

$$\boldsymbol{v}_p(\boldsymbol{k},\omega) = \frac{\omega}{k}\boldsymbol{u}^* \quad (8)$$

Where $\boldsymbol{u}^*$is the unit vector in the direction of the wave vector k = $|\boldsymbol{k}|$ [61].

Phase velocity is represented in many ways. Contour plots are the most used to describe the phase velocity information.

Group velocity, which gives the information about the speed of the entire wave packet and its direction of propagation, is known as the group velocity. We know that energy is propagated in the form of waves. The direction of the energy flow in any wave is equal to the direction of the group velocity [62]. It not only speaks about a single wave but, gives us complete information about the entire wave packet. Group velocity also knows as group speed is

$$\boldsymbol{v}_g(\boldsymbol{k},\omega) = \frac{\partial\omega}{\partial k_1}\boldsymbol{i}_1 + \frac{\partial\omega}{\partial k_2}\boldsymbol{i}_2. \quad (9)$$

Where k_1 and k_2 are the wave vectors in x and y directions.

It is obtained by considering the variations of the wave vector with respect to the frequency in both x and y directions.

Group velocity is also represented using contour plots. We have other important ways to represent and observe the direction of energy flow through group velocity plots, which speak about the directionality of the waves.

When we compare the phase and group velocity, phase velocity tells the speed of any single wave in a wave packet, whereas the group velocity gives the information about the speed of the wave packet and also the direction of the energy flow. The information about the direction of the waves is majorly considered in the current work because of the advantages of using it to study the "directionality" of the waves. So, group velocity gives us more information in terms of the direction of the wave than phase velocity as shown in Figure 8, Figure 9, Figure 10.

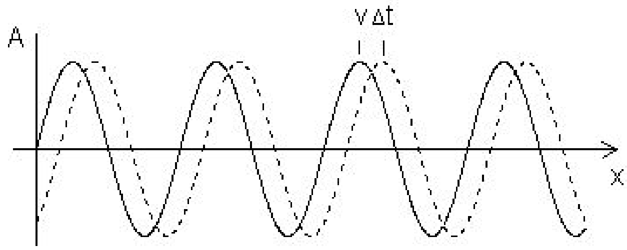

Figure 8. Wave with forwarding shift (change in phase of the wave).

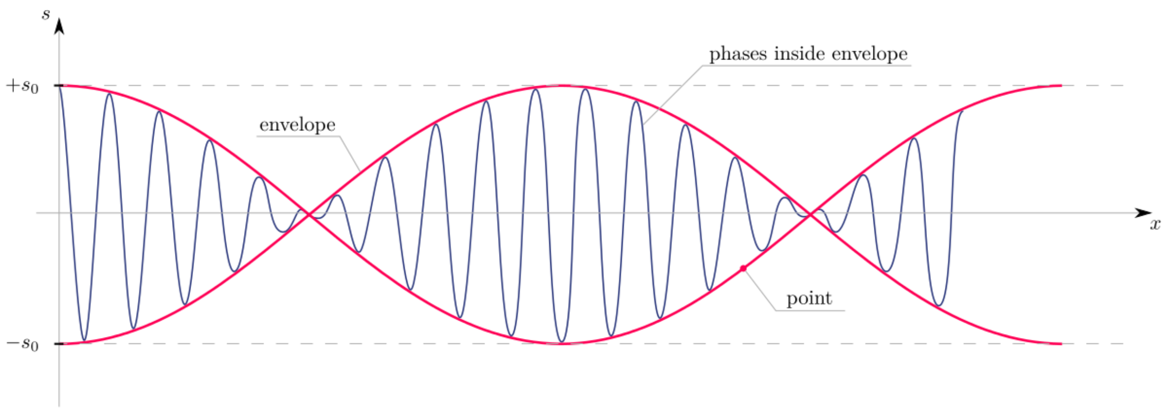

Figure 9. Phase and the group velocity with envelope

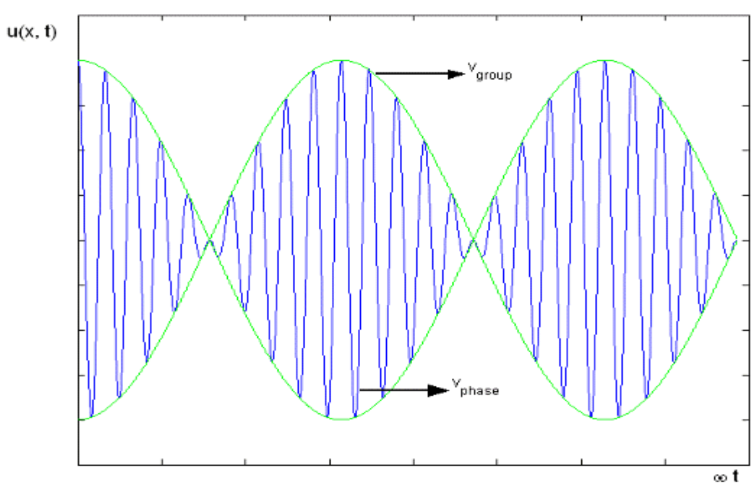

Figure 10. Phase and the group velocity [62]

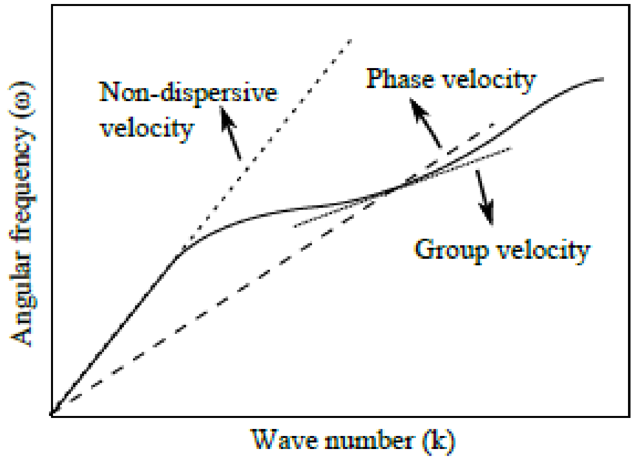

Figure 11. The dispersion relation for a dispersive medium. The solid black line represents the dispersion curve, the phase velocity is the slope of the secant cutting the curve and the group velocity is the slope of the tangent in that cutting point [30].

From the picture above, we see the green line (envelope) which is covering all the small waves inside is the envelope representing the group velocity of the wave packet. The blue waves present inside travel with the phase velocity. The wave packet moves at the group velocity [62].

When the phase speed is constant with respect to the frequency, the wave is non-dispersive. In a non-dispersive medium, **k** and ω are proportional. In this case, the phase velocity is equal to the group velocity.

2.2.3 Wave directivity

Wave directivity refers to the directional energy flow in the lattice structure. Waves travel in different directions in different kinds of media. The ability to control their directional behavior is called "wave directionality." It merely means that we can control the direction of the wave propagation and tailor it accordingly.

According to the study of wave propagation, most of the directional properties of a wave are derived from its group velocity. So, in the current study, we inspect the directionality of the wave propagation through the group velocity of our considered structure. Additionally, we also investigate the bandgaps (the portion where the propagation of the waves at a particular range of frequencies is prevented).

So, from the concepts of directionality, we can investigate the directional behavior of the waves and tailor them according to our needs, including the tailoring of the bandgaps.

Graphical representation of the directional behavior of waves

We study the directional behavior of the waves in many ways, such as (a) iso-frequency contour plots, (b) group velocity contour plots and polar plots for group velocity.

The iso-frequency contour plots are also known as the phase-constant surfaces. Based on the finite element analysis of free wave motion, the variation of the frequency with respect to the wave vectors k_1 and k_2 (in x and y direction) results in the iso-frequency contour plots. They show the relationship between the frequency and the wave vectors from which we can observe the directional properties of the wave propagation.

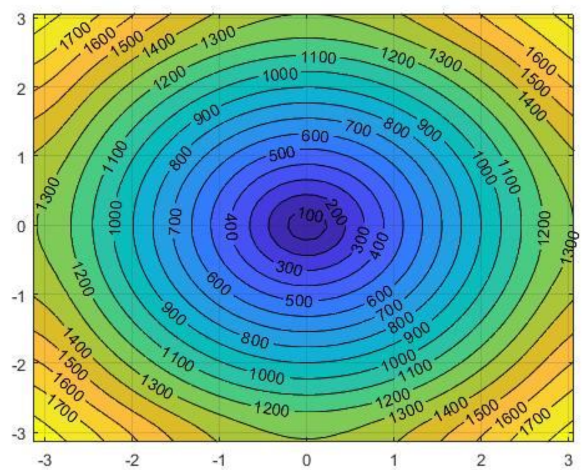

Figure 12. Iso-frequency contour plot.

Each line inside the plot represents an individual frequency. The direction perpendicular to each contour lines indicates the direction of propagation for that particular frequency. By drawing the perpendicular vectors to all the iso-frequency contour lines, we can see the directional behavior of all the frequencies present.

The contour plots can also represent the group velocity. We use the equation of group velocity (Equation.9) to plot these. We take the required data from the iso-frequency contour plots such as the information about the wave vectors and the frequency and plugging them in the group velocity gives the chance to plot them in the same way.

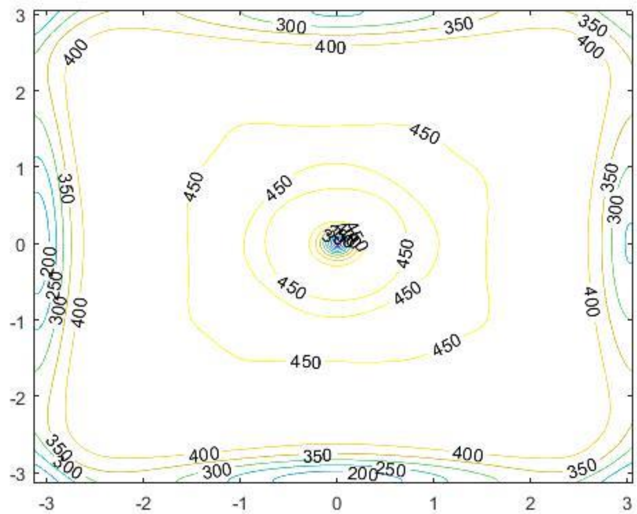

Figure 13. Group velocity contour plot.

From the plot above, we see all the frequency lines. Considering a point in any one of the frequency lines, the distance of the point from the center gives the directional behavior in that particular direction. In the picture, we see that the diagonal ends are far away when compared to the other portions of the plot. This means that most of the wave propagation is in the direction of the diagonals.

Polar plots:

The perception of the directional conduct of the wave propagation utilizing polar plots is exceptionally fascinating and helpful. As indicated by Ruzzene [23], fitting continuous functions to the iso-frequency contours and differentiating it gives us the outcome for group velocity. Be that as it may, to improve it, we utilize an improved philosophy to break down the group speed dissemination [63]. Utilizing a polar plot is better in understanding the directionality of the waves in 360° and the magnitude of those waves in that particular direction. The frequency takes the radial axis, and the theta pivot demonstrates the direction of the wave inside the structure.

In this way, every one of the portrayals talked about above are incredibly helpful in discovering the conduct of wave directionality. It is anything but difficult to contemplate the directivity of the waves in various ways utilizing every technique as indicated by the circumstance. The most effective way to represent the group velocity magnitude and direction is by using the polar plots. Every single plot that appeared above has its very own importance and use. All these can be utilized to tailor the directional conduct of the waves in required directions with the required magnitude for a picked structure. More details on polar plots are clarified in section 3.5

Chapter 3

3. METHODOLOGY

In this section, we examine the procedure utilized in deciding the directionality of the waves in square hierarchical lattice structures. Bloch periodic boundary conditions are utilized to comprehend the numerical investigation, and the participation factors are used to decide the in-plane and the out of plane waves in detail. Likewise, utilizing the polar plots to examine group velocity is exhibited.

3.1 Unit cell configuration

The unit cell is the littlest repeating unit in a periodic structure. A periodic structure is an accumulation of unit cells stacked alongside one another with the end goal that they do not overlap [59]. In a periodic structure, a unit cell with the minimum area is known as a primitive unit cell.

The unit cells considered in this research are taken from [59]. A square lattice (as shown in Table 2(a), which then modified as a hierarchical lattice by adding sub-structures at the intersection, is shown in Table (2). Apart from the simple square lattice, two different first-order hierarchical lattices have been considered: One self-similar hierarchical lattice structure as shown in Table 2(b) – Square in a square hierarchical lattice structure and one non-self-similar hierarchical lattice structure as shown in Table 2(c) – Hexagon in a square hierarchical lattice structure. From Table (2), the structural organization of hierarchical lattices is defined by the characteristic length ratio [64, 65]. $\Upsilon = \mathrm{r}/\mathrm{L}$ is the proportion of recently introduced hierarchical edge length to the previous hierarchical edge length. 'L' is the side length of zero-order lattice, and 'r' is the edge side length or radius of the first-order hierarchy. Relative density $\rho_0 = \rho_c \rho_s$ of the structure is the ratio of the density of the cellular structure to the density of the solid. 't' is the thickness, which is assumed to be uniform through the structure. All the unit cells considered are normalized with a structure similar to the square lattice of fixed-fixed boundary condition in the horizontal direction and roller boundary condition in the vertical direction.

Table 2. Unit cells and their respective irreducible Brillouin zones [59]

Lattice	Unit cell	Respective IBZ
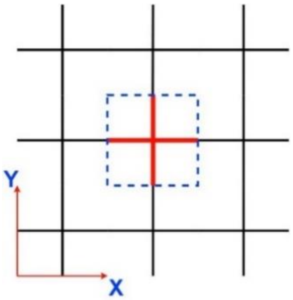	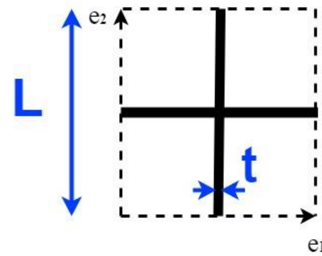	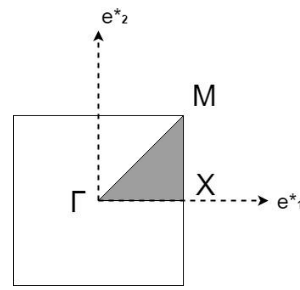
(a) Square lattice		
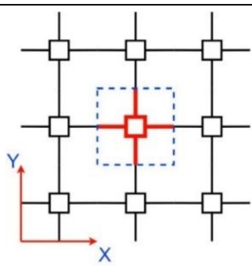	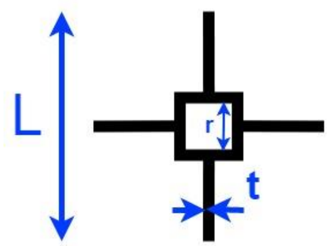	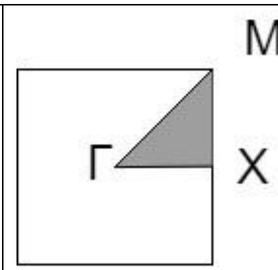
(b) square in a square hierarchical lattice		
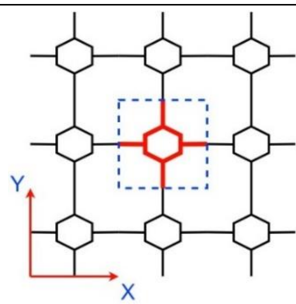	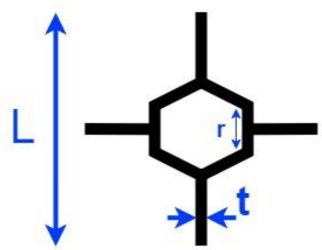	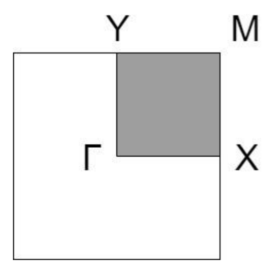
(c) Hexagon in a square hierarchical lattice		

As discussed before, we do not let the wave vectors to sweep over a specific path in the Brillouin zone. Instead, a 25/25 grid, as shown in Figure 14, is what is followed here to sweep the entire first quadrant of the Brillouin zone. All the k_x, k_y points are considered inside the zone, calculating the frequencies at each point.

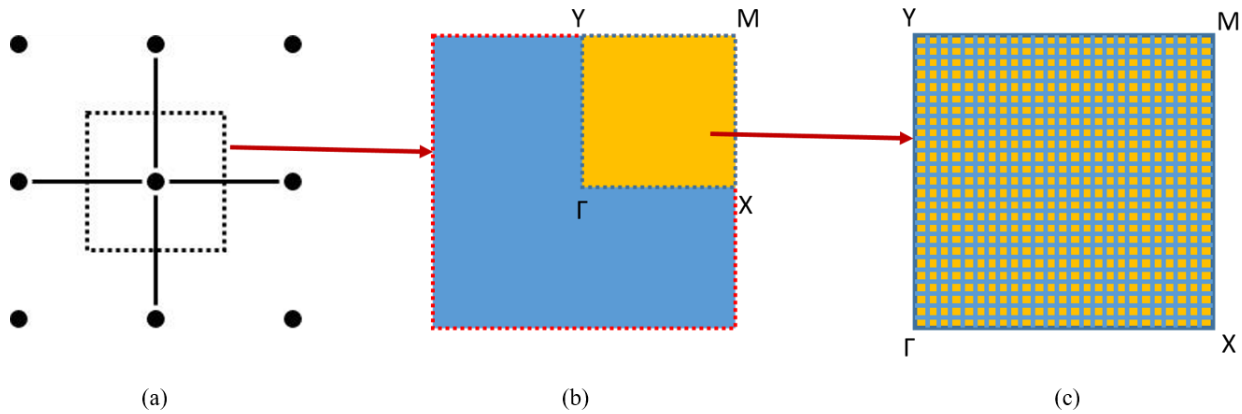

Figure 14. (a) Brillouin zone of a square lattice (b) First quadrant in the Brillouin zone (c) 25/25 grid indicating all the k_x, k_y points considered.

3.2 Floquet Bloch periodic boundary condition

3.2.1 Wave propagation in periodic media

Wave motion through a periodic system is analyzed using Bloch's theorem. It states that the proportionate change in wave amplitude occurring from cell to cell does not depend on the cell location within the periodic system [23]. As per Bloch's condition, when an infinite periodic lattice is considered, a unit cell taken is sufficient to get the characteristics concerning the wave qualities of the whole structure. In Comsol, we select the source point and the destination point in the unit cell. Bloch's theorem relates the displacements in the source and the destination by [55]

$$U_m(r) = U_m\big(r_{RUC}(r)\big)\exp\left[ik.\big(r - r_{RUC}(r)\big)\right] \tag{10}$$

$$U_m(r) = U_m\big(r_{RUC}(r)\big)\exp\left[ik.\sum_{\alpha=1}^{d} n_\alpha e_\alpha\right] \tag{11}$$

Where the wave vector is $\mathrm{k} = \mathrm{k}^{\mathrm{Re}} + \mathrm{k}^{\mathrm{Im}}$ From the above equation. The real part of the wave vector is the attenuation constant, and the imaginary part is called phase constant, and the attenuation constant here is set to zero because no material-inherent losses are assumed. So, $\mathrm{k} = \mathrm{k}^{\mathrm{Im}}$.

Each point r is connected to a point $\mathrm{r}_{\mathrm{RUC}}$ in the reference unit cell by the notion of periodicity,

$$r - r_{RUC} = \sum_{\alpha=1}^{d} n_\alpha e_\alpha \tag{12}$$

With integers $\{n_1 \ldots . n_d\}$

Thus the displacement of any point in the considered cross-section is [55]

$$u_m(r,t) = U_m\big(r_{RUC}(r)\big)\exp\left[i\left(k^{Im}.\sum_{\alpha=1}^{d} n_\alpha e_\alpha - \omega t\right)\right] \tag{13}$$

3.2.2 Eigenvalue problem

Bloch's periodic boundary condition is utilized in finite element modeling. The standard element procedure for unit cells equation of motion is:

$$M\ddot{U} + KU = F$$

Where M and K are the global mass and global stiffness matrices of the unit cell. F and U are the global force and displacement vectors. Considering

$$U(t) = \widehat{U}\exp\,(i\omega t) \tag{14}$$

And

$$F(t) = \widehat{F}\exp\,(i\omega t) \tag{15}$$

We arrive at

$$(\mathrm{K} - \omega^2 M)\widehat{U} \;= \widehat{F} \tag{16}$$

For the analysis of free wave motion, F = 0. So,

The reduced eigenvalue problem is

$$(\mathrm{K} - \omega^2 M)\widehat{U} \;= 0 \tag{17}$$

From this, we solve our dispersion relation $\omega = \omega(k)$ from which we will be able to associate the frequencies concerning the wave vectors.

From the dispersion relations, we calculate our phase velocity:

$$V_p(\mathbf{k}, \omega) = \left(\frac{\omega(k)}{k_1^{Im}}, \frac{\omega(k)}{k_2^{Im}} \right)^T \tag{18}$$

Also, the group velocity as:

$$V_g(\mathbf{k}, \omega) = \left(\frac{\partial\omega(k)}{\partial k_1^{Im}}, \frac{\partial\omega(k)}{\partial k_2^{Im}} \right)^T. \tag{19}$$

$$V_g(\mathbf{k}, \omega) = \left(V_{gx}, V_{gy} \right)^T. \tag{20}$$

$$ϟ = \sqrt{\left({V_{g_x}}^2 + {V_{g_y}}^2 \right)}. \tag{21}$$

Where ϟ iis the magnitude of the group velocity.

3.3 Finite Element Analysis

In this study, the commercial finite element package Comsol Multiphysics is utilized to analyze the hierarchical structures. The structures are modeled using 3D Timoshenko beam elements to display the cross-section structures with six degrees of freedoms — three translation (u, v, w) and three rotational (θ_x, θ_y, θ_z) degrees of freedom.

In Comsol, we use the Floquet Bloch periodic boundary conditions utilizing the linear extrusion operator. We utilize the definitions tab to include the participation factors and the mass properties for the selected structures. Beam physics is selected from the specified interface section in Comsol. The participation factors and the mass properties are later used to separate the surfaces as in-plane and out of the plane. Here, we talk about the procedure used in Comsol to estimate the participation factors and the general mass of the structure used for the picked eigenfrequencies, as shown in Figure 15. and Figure 16.

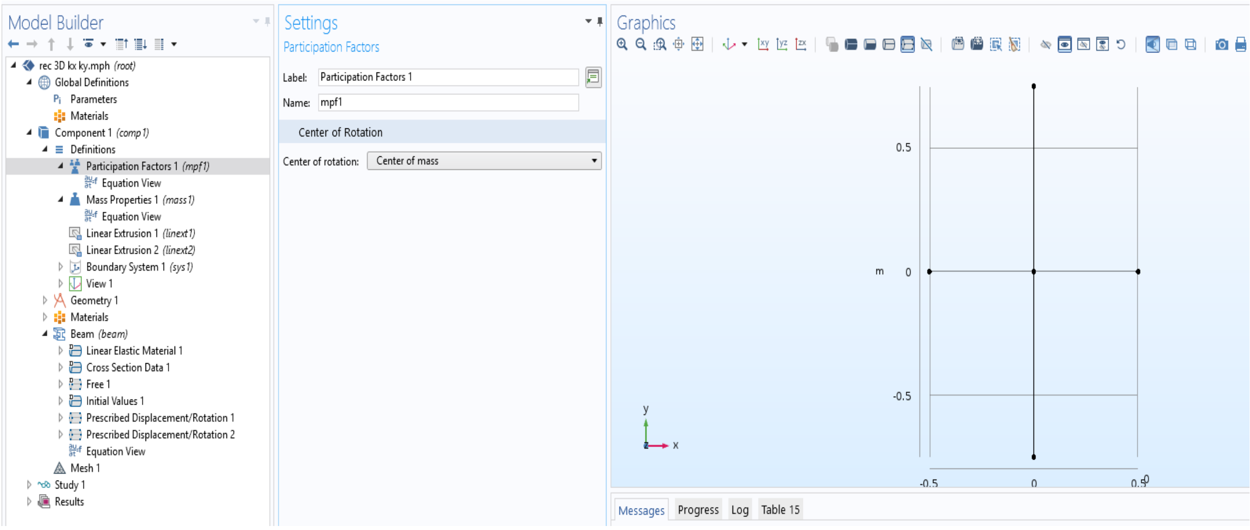

Figure 15. Participation factor tab in Comsol multiphysics software

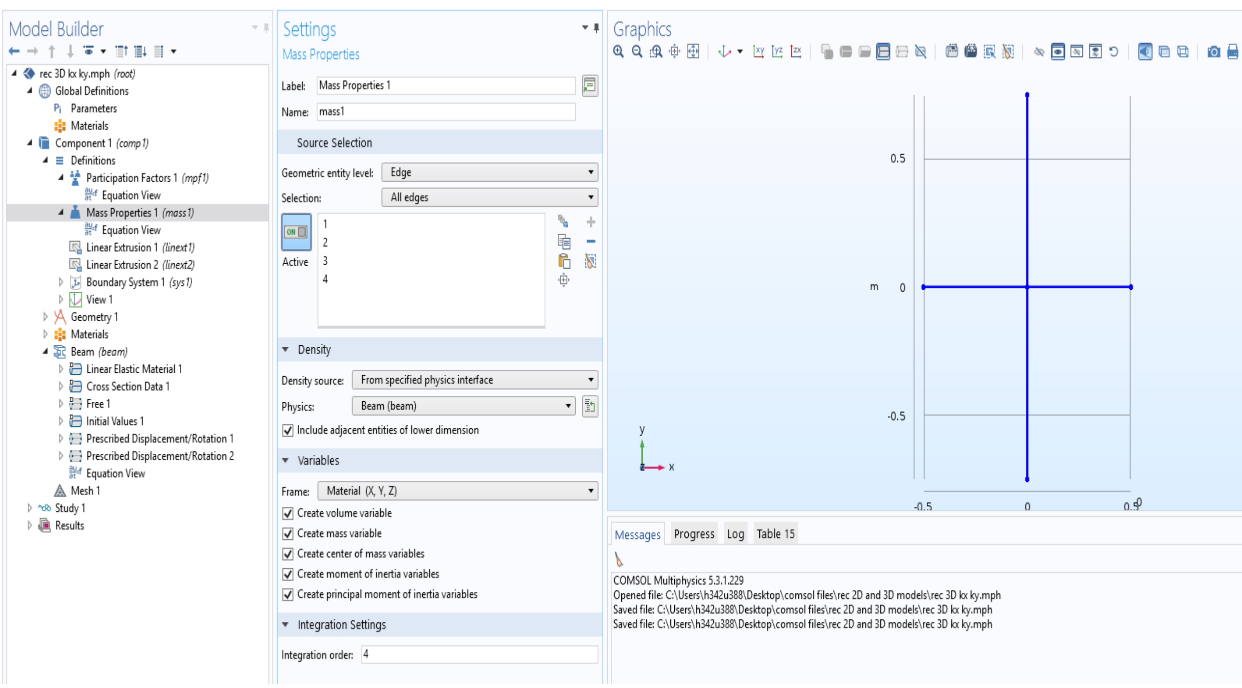

Figure 16. Mass properties selection in Comsol

From the density source, we pick the specified physics interface to choose the physics to be beam-type since all the edges are beam elements.

We simulate the model for 25/25 steps as per the right Brillouin zone applied. Upon completion, the data obtained is exported from Comosl to Matlab. In the outcomes (results) tab, we can extract the data out from the "derived values." From global evaluation, we can approach the software for the necessary information, which turns out in a table configuration, as shown below in Figure 17.

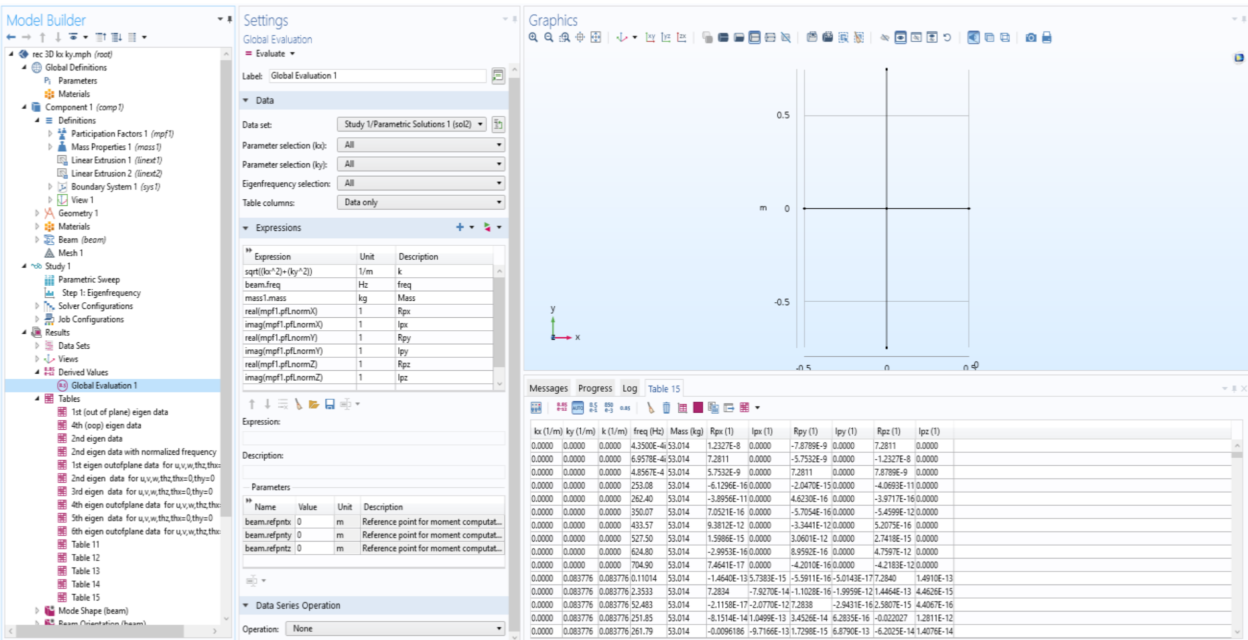

Figure 17. The global evaluation tab is shown with the tables derived from Comsol.

3.4 Modal participation factors

In a vibration's perspective, any structure when vibrated gives us the eigenvectors and the eigenmodes. Eigenvalues or eigenvectors represent the natural frequencies of the framework at which it vibrates, and the eigenmodes demonstrate to us the displacements of the structure in different directions. These displacements maybe along the line of axis or opposite to it. As discussed in chapter 2, P mode and S mode are separated by the type of displacement concerning the axis. So we watch both longitudinal and flexural movements inside and out of the plane in a lattice structure. These are classified as the in-plane and the out of plane modes. The dispersion surfaces identified with these are known as the in-plane and the out of plane surfaces.

3.4.1 In-plane & out of plane surfaces

In the present work, the wave vectors are swept over the Brillouin zone in all the models for 25/25 steps in x-direction and y-direction. With this methodology, we limit the arrangement of wave vectors to be researched just along the Brillouin zone and make the procedure more accurate and generalized. An in-plane surface speaks to the information containing the frequencies which are related to the displacements occurring inside the structure. Thus, the out of plane surface speaks to the focuses with frequencies related to the displacements outside the structure.

Dispersion surfaces are the 3D portrayals of the dispersion curves. They comprise of the frequencies with their regarded k_x and k_y points. The surfaces got for each model contain the information which involves the in-plane and out of plane wave motions. They are filtered and isolated by the in-plane and out of plane criteria, which is clarified in the following segment. They are utilized to make new surfaces, which are known as the in-plane and out of plane dispersion surfaces.

3.4.2 Participation factor & the beta factor

Modal participation factors are scalars that measure the interaction between the modes and the directional excitation in a given reference frame. Larger values indicate a stronger contribution to the dynamic response [66]. Modal participation factors are essential in deciding the importance of the vibration of a specific mode. In the present work, we use α to mean a mode. Each structure has its mass, and the generalized mass of the structure for a specific mode α is: [67]

$$m_\alpha = \psi_\alpha^T M \psi_\alpha \tag{22}$$

Where M is the structure's mass matrix and ψ_α is the eigenvector of that specific mode.

Eigenvectors can be normalized in different kinds. The eigenvectors can be scaled, so the largest entry in every vector is solidarity, or they can be normalized with the goal that the generalized mass for every vector is unity (m_α= 1). The decision of normalization does not impact the outcomes; however, it decides the way wherein the eigenvectors are represented.

The participation factor for mode α in direction i, $P_{\alpha i}$ is a variable that shows how unequivocally motion in global x-, y-or z-direction, or rotation about one of these (indicated by i, i=1,2,3…,6) axes is represented in the eigenvector of that mode. It is

$$P_{\alpha i} = \frac{1}{m_\alpha} \psi_\alpha^T M T_i \tag{23}$$

Where T_i means the magnitude of the rigid body response to the imposed degree of motion in the i-direction.

Presently, to separate between in-plane and out of plane modes, we calculate a scalar in-plane ratio [55]

$$\beta = \frac{\sqrt{P_1^2+P_2^2}}{\sqrt{(P_1^2+P_2^2+P_3^2)}} \qquad \rightarrow \qquad \beta = \begin{cases} 1 & \text{for in} - \text{plane modes.} \\ < 1 & \text{for out of plane modes.} \end{cases} \tag{24}$$

Where P_1, P_2 & P_3 are the participation factors in the directions x, y, and z.

And $0 \leq \beta \leq 1$.

3.4.3 Prior results

In [59], we examine the generation of bandgaps from the impacts of structural and material symmetry. Waves are separated as P and S utilizing the participation factors. We see the generation and tuning of bandgaps by changing the properties of the geometrical and material symmetries. The width of the bandgaps and the location of the bandgaps are additionally tuned. We identify from [59] that structural symmetry in first-order hierarchical lattices plays a vital role in the bandgap arrangement. We observe a significant distinction regarding bandgap width and its position between the structurally symmetric and asymmetric hierarchical lattice structures. As the asymmetry increases, the width of the bandgaps diminishes, though the quantity of bandgaps increments. Material asymmetry is utilized to uncouple the coupled bands, which results in the generation of bandgaps. Slender bandgaps are made at lower frequencies because of material asymmetry, and the broader bandgaps are held because of the structural symmetry.

All the work from [59] is focused on the in-plane dispersion properties of various hierarchical lattice structures. Out of plane qualities are neither centered nor considered. Directionality is another essential idea that is disregarded in [59]. In current work, the essential center is moved towards the directionality conduct of in-plane and the out of plane dispersion properties. We examine the strategies to separate in-plane surfaces and the out of plane surfaces, including the directional behavior of the surfaces exclusively and together. In this work, we attempt to find the bandgaps utilizing the group velocity magnitude and their course by considering the direction of the group velocity.

3.4.4 Verification

As discussed in section 3.1, we take the data related to the model, which comprises of the wave vectors and the frequencies, including the mass of the framework and the participation factors. We plug the participation factors in Equation.22, and we get the values for the beta factor, which are between 0 and 1. From this, we get every one of the information required to plot the dispersion surfaces. We can plot the general dispersion surfaces which have the data related to all the motions and plot the required in-plane and out of plane dispersion surfaces extracted from them.

The general dispersion surfaces for a rectangular model are appeared in [63] are shown in Figure 18. The model is picked to determine the initial three out of the plane and in-plane surfaces and the group velocity polar plots. The same steps from [63] are pursued without frequency and wavevector normalizations, and the outcomes are demonstrated as follows.

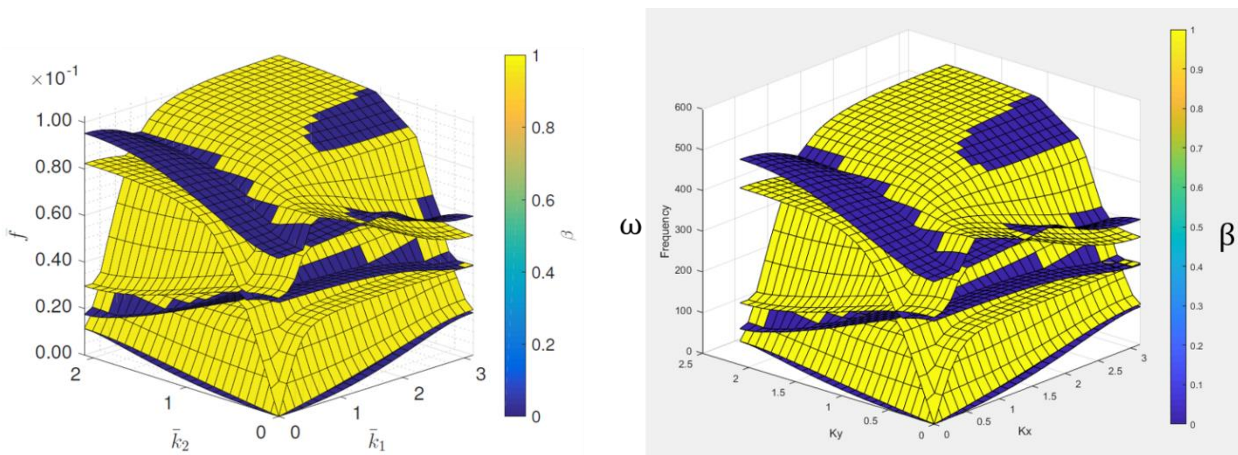

Figure 18. (a) Dispersion surfaces [63] (b) Results from Comsol data

Figure 18. Demonstrates the comparison between the outcomes from [63] and the outcomes from Comsol. From the Figures, we see that the surfaces are yellow in shading when the estimation of beta is one and purple when it is zero. This process isolates the part with the in-plane information with the out of plane information.

Representing the surfaces with in-plane and out of plane data points using the beta factor is finished. Presently, we need to focus on extracting the information required to create a new surface.

From the surfaces got above, we extricate the out of plane information required to assemble the first out of the plane surface. The first dispersion surface obtained is entirely out of the plane, which does not require any extraction of information, as appeared in Figure 19. However, for the second out of the plane surface, we need to choose surfaces 2, 3, 4 from Figure 20. and extract all the purple information which relates to the out of plane wave motion and add that information to create a new surface as appeared in Figure 21. All the information that stayed in the wake of making a surface is utilized in creating the next surface.

For instance, after making the initial two out of plane surfaces, some part of surface 4 in Figure 22. belongs to another wave propagation mode, which is why it is left behind without being used. So to make a third out of the plane surface, we use this unused information from the fourth dispersion surface and include it with the data from the fifth and the sixth dispersion surface to make the third complete out of the plane surface, as appeared in Figure 23.

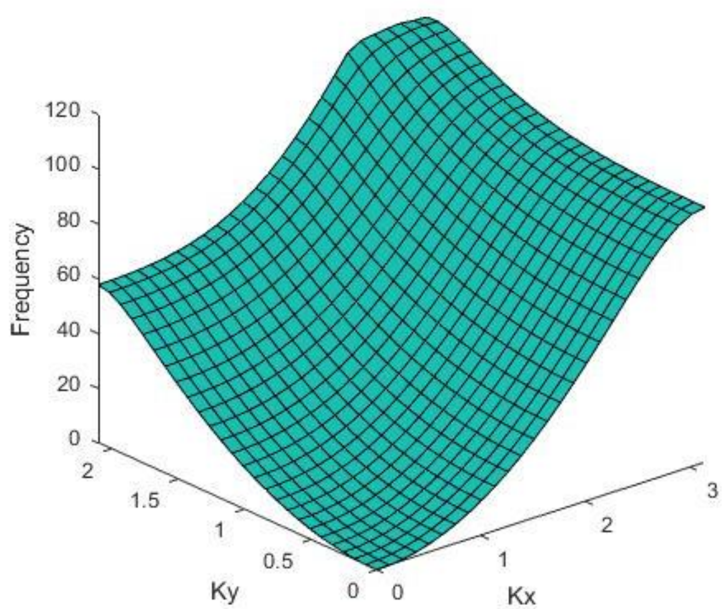

Figure 19. First out of the plane surface in the rectangular lattice.

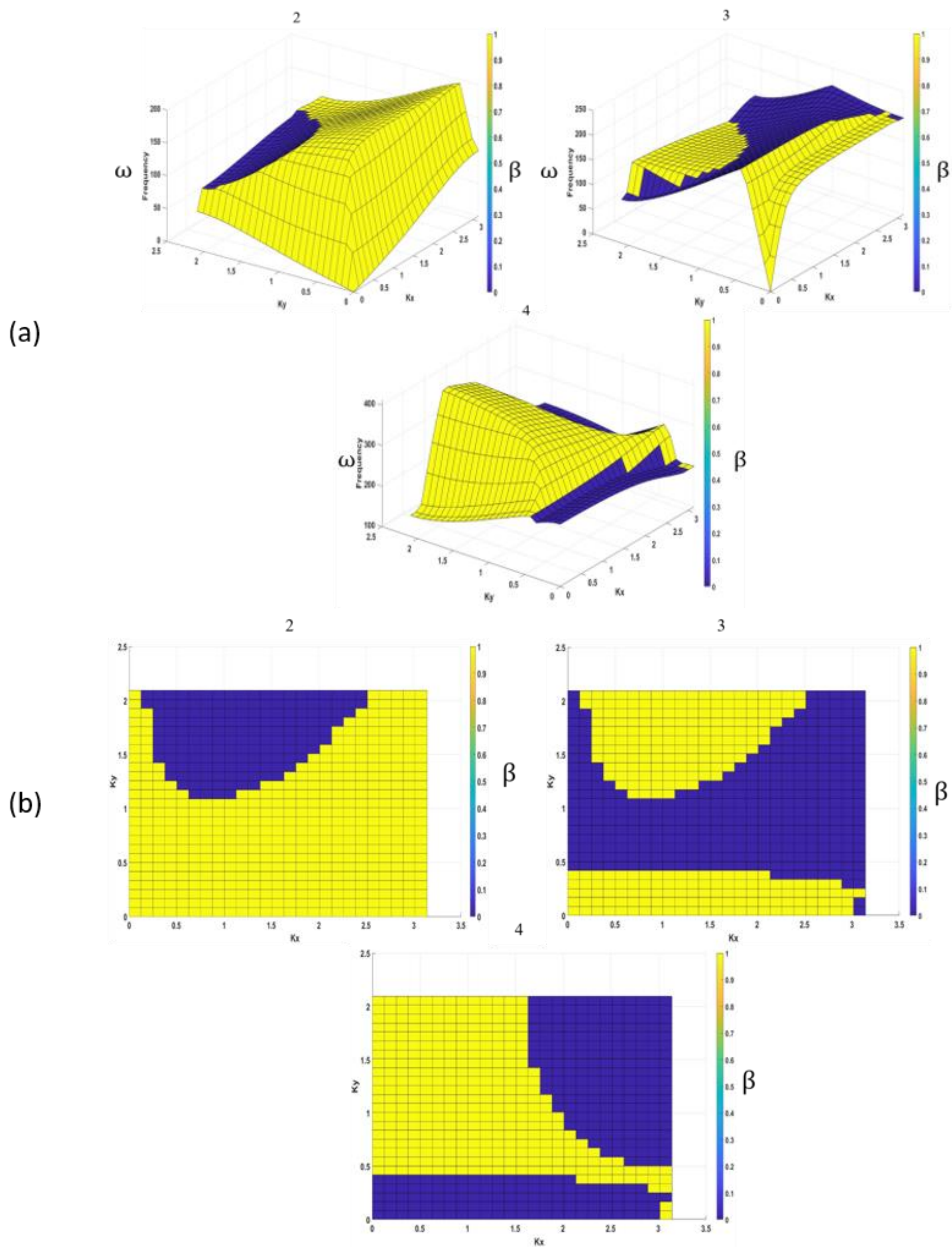

Figure 20. Rectangle (a) 3D view of 2,3,4 dispersion surfaces (b) 2D view of 2,3,4 dispersion surfaces.

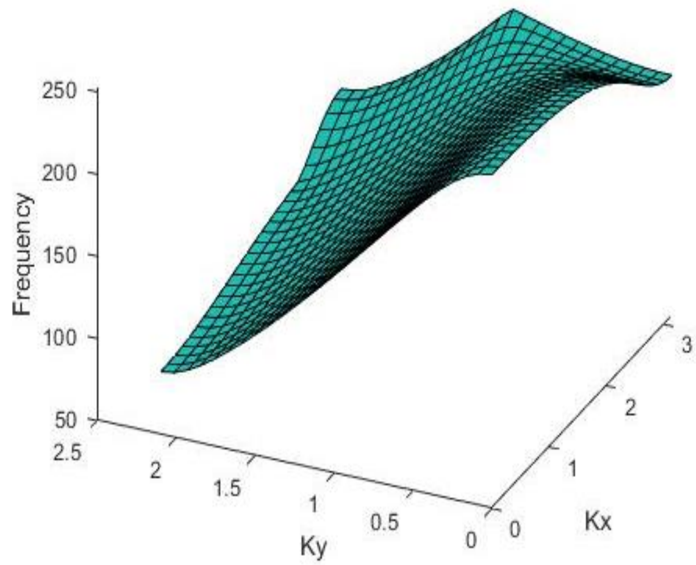

Figure 21. Second out of the plane surface.

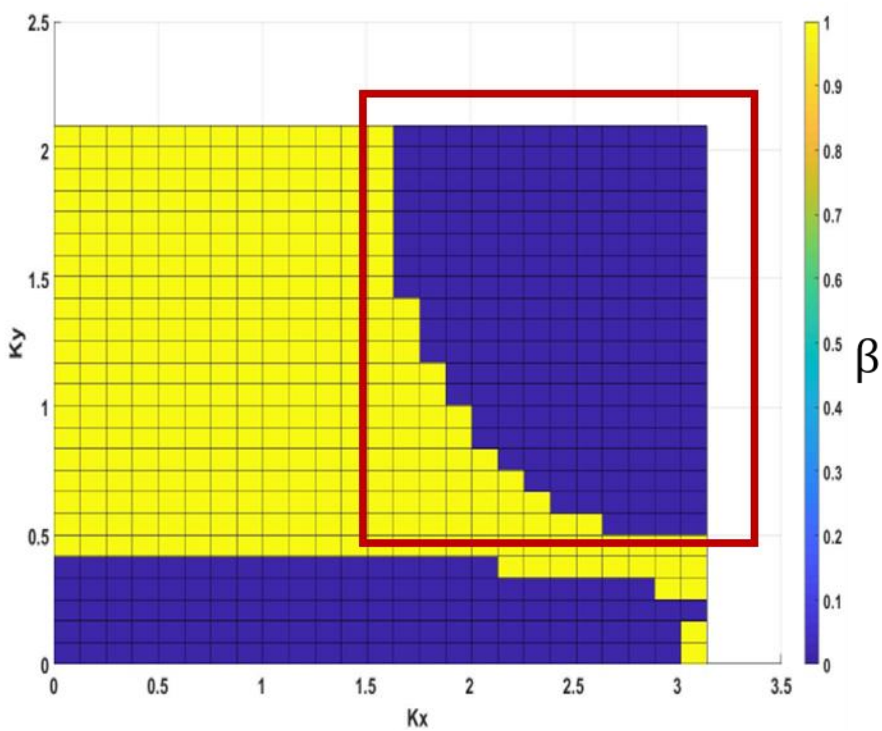

Figure 22. Unused out of plane data from the fourth dispersion surface

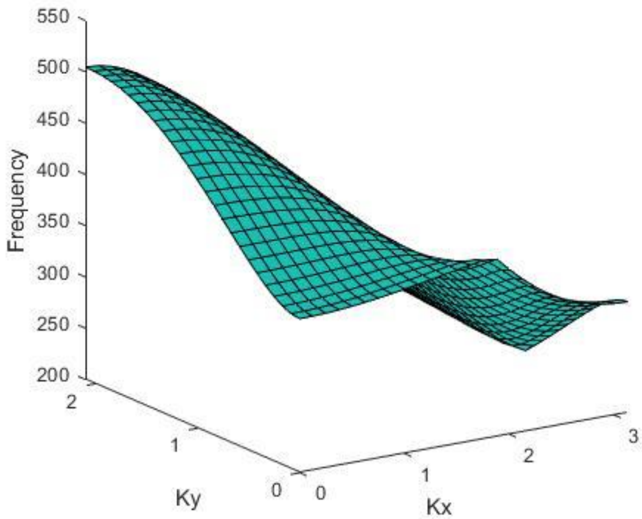

Figure 23. Third out of plane surface

In-plane wave propagation

Out of plane wave propagation

3.5 Polar plots

3.5.1 Introduction

A polar plot is a plot, which is utilized to express a function in polar coordinates, with radius r and angle (theta). Here, they are drawn between the magnitude and phase of the group velocity as a function of frequency. A general polar plot resembles Figure 24.

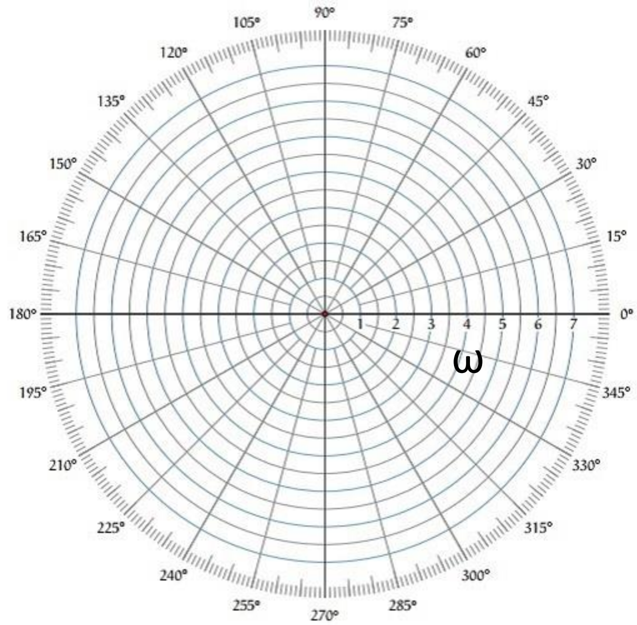

Figure 24. Polar plot representation.

n the present work, the radial axis speaks to the frequency of the system, and the theta hub represents the direction in which the velocity of the system exists or travels.

The polar plots shown in this research work are from 0° to 90° since all the structures we consider are in symmetry with the first quadrant, we choose to show the group velocity direction and magnitude in that range.

From this, we comprehend that by utilizing the polar plot to represent the group velocity, we can obviously show the extent of the group velocity at a specific point and its existence in that particular direction concerning the frequency of the structure in that area.

3.5.2 Procedure

The determination of group velocity evolutes from the dispersion relations. The gradient of the dispersion surfaces brings about group velocity. Be that as it may, utilizing dispersion surfaces that are obtained by following the K-space, which is restricted to a particular path of the Brillouin zone, gives us less information about the group velocity, which would be not accurate.

A conventional method to assess the group velocity is by utilizing the iso-frequency contour plots of the dispersion surfaces. But, in this way, the magnitude and the direction are not uncovered accurately. So from [23], fitting continuous functions to the iso-frequency contour plots result in a better approximation of the group velocity. The scope of free wave movement is assessed by evaluating the function ($k_y = f(k_x)$ defining a given iso-frequency contour line in the first quadrant. For a considered unit cell, the direction of the wave propagation phi is

$$\emptyset = \tan^{-1}\left(\frac{\mathrm{L_y}}{\mathrm{L_x}} * \frac{\mathrm{V_{gy}}}{\mathrm{V_{gx}}}\right) \tag{25}$$

Lx and Ly are cell dimensions in x and y directions. Since we have a square structure, they are always 1 [m] as considered.

As appeared in Figure 25, which is a correlation of the first out of the plane surface of a rectangular model from [55] is a guide to watch the group velocity by following the above strategy.

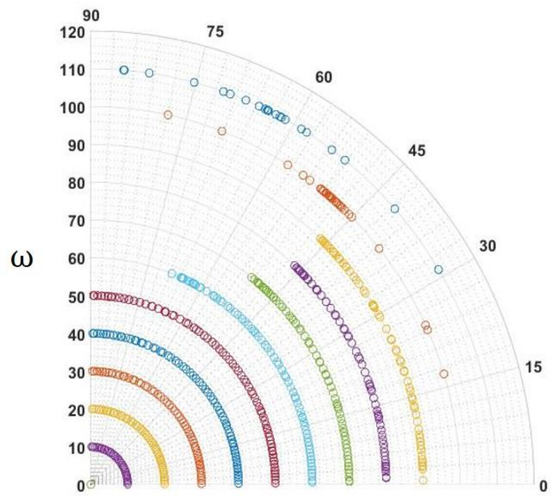

Figure 25. Polar directivity plot for the first out of plane surface for the rectangle

An improved strategy to break down group velocity [55] is utilized in the present work. So in this, we pursue a procedure to compute group velocity at every point inside the structure using a 25/25 matrix as examined before to cover the whole quadrant in the square structure chosen. From this, we get a plot with continuous maps of group velocity, showing its magnitude and the direction with respect to the frequency. The **modulus** of the group velocity gives the magnitude of the group velocity. This **magnitude** is plotted with respect to the frequency and the direction of wave propagation to give us a continuous map of the velocity. Adding magnitude to the directivity plot gives us the directionality plot.

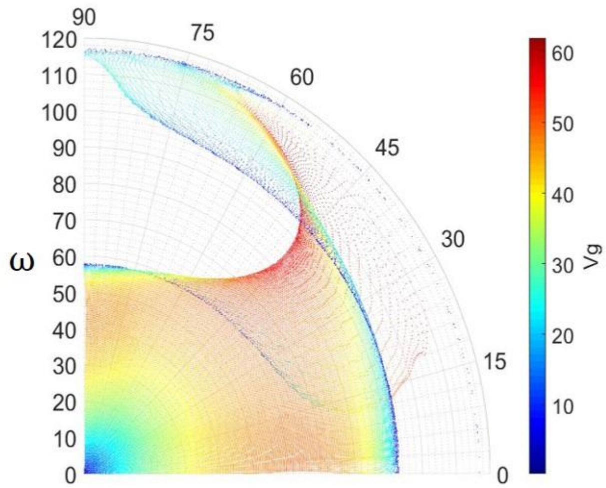

Figure 26. Group velocity map for the first out of plane surface of the rectangle.

A rectangular structure [55] is picked, and its group velocity results for the first and second out of plane surfaces are demonstrated separately and together. Figure 26. shows the group velocity for first out of the plane surface of the rectangular model, which is the improved portrayal of Figure.24. The comparison of the group velocity plots for the first two lowest out of plane surfaces appears in Figure.27.

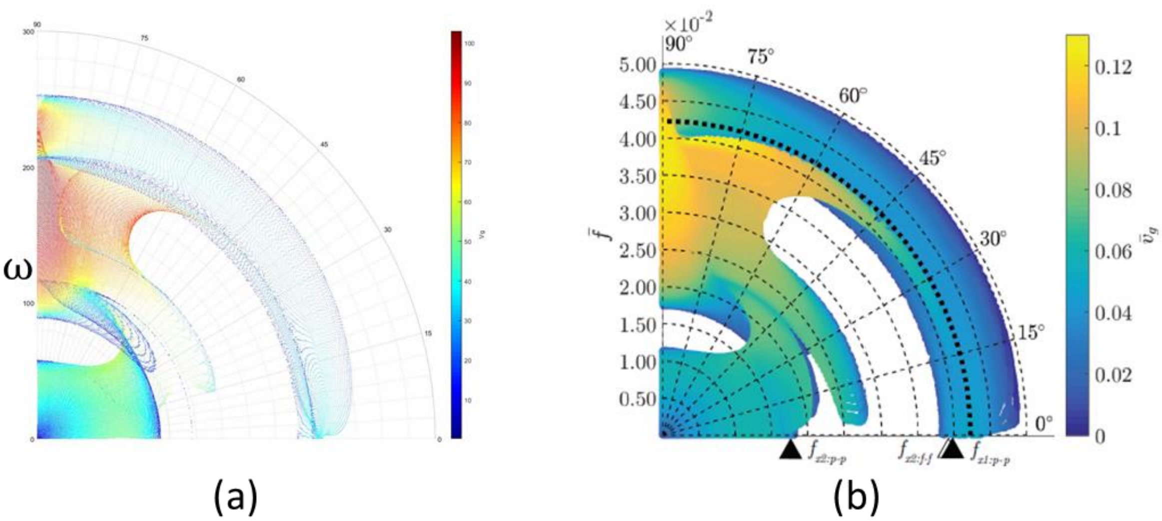

Figure 27. (a) Group velocity for the first two out of plane surfaces replicating (b) Same result from [55]

3.5.3 Importance

Group velocity can be spoken to in numerous kinds. Many research works use contour plots to portray group velocity direction, which entirely relies on the frequency determination and the dispersion relation, as clarified previously. The group velocity contour plots don't give away a lot of data on the group velocity since they correspond to a path covering the Brillouin zone. They principally rely upon the decision of frequency and don't show the whole magnitude and the course of the group velocity in a solitary plot.

Utilizing a polar plot to portray group velocity has numerous points of interest. We can see the magnitude and the direction of it regarding the frequency. We can locate the bandgaps quickly and can decide the directionality of the wave motion by the position of the bandgaps. Along these lines in this work, we utilize the polar method for portrayal to show the location of bandgaps and the variety of the group velocity at each point concerning the frequency which is called as the “Wave Beaming.” In view of the outcomes acquired, we will have the option to know the directionality of the structures in a proficient way.

In the present work, we consider three different square hierarchical structures to study the directionality. The investigation isn't merely founded on the in-plane surface information yet, also, considers the out of the plane wave motion to describe the whole behavior of the structure. We display the dispersion surfaces of each structure as required and show the polar velocity plots to depict the directional properties of that specific mode for that picked structure. Segment 4 comprises of the outcomes identified with the group velocity for all the structures. Section 5 depicts the dispersion surfaces used to make and separate the in-plane and out of the plane surfaces and clarifies the directionality conduct dependent on the bandgaps.

4. RESULTS & DISCUSSIONS

In light of the parameters and calculations, we attempt to discover the directionality conduct of the basic square, square in a square, and the hexagon in square lattice structures. In this segment, we focus on demonstrating the idea of wave beaming and directionality through the dispersion bands, dispersion surfaces, and the polar plots to depict the group velocity. We consider 35 surfaces for each structure out of which we infer 15 in-plane and out of the plane surfaces in examination with dispersion curves. We use 3D structures to acquire the data related to the out of plane wave motions.

All the Figures with the dispersion curves in this section are taken out from the 2D and 3D models following the Brillouin zone, as explained in chapter 3. However, to increase the accuracy of the outcomes and make a more generalized study on the structures, a 25/25 grid, as explained in chapter 3, is followed to increase the size of the study by increasing the number of points considered. At last, the polar plots are appeared to show the whole data identified with the wave directionality depicting the bandgaps, variety of the velocity, and partial bandgaps dependent on the kind of structure.

4.1 Simple square lattice structure

4.1.1 In-plane dispersion curves

A simple square structure has no level of the hierarchy Figure 28. shows the band diagram for the first 15 dispersion bands normalized with 205.85Hz according to [59]. The frequency of the boundary condition chosen is ω_0. The normalized frequency is $\left(\acute{\omega} = \frac{\omega}{\omega 0}\right)$. We see the bandgaps from the dispersion curves. This band diagram uncovers the data on all the in-plane wave motions which occur inside the square structure.

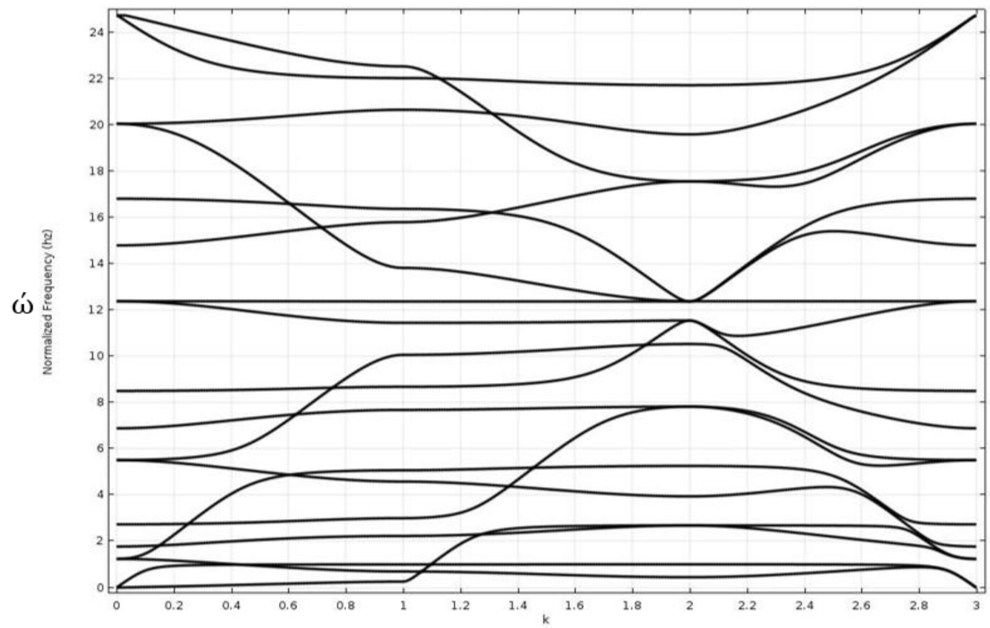

Figure 28. Square dispersion curves – in-plane

4.1.2 In-plane & out of the plane dispersion curves

Discussing the out of plane wave motions for the same structure, when we consider the wave motions which are perpendicular to the plane of the structure, we watch some more bands in a similar scope of frequency because of the incorporation of the out of plane wave motions. These appear in Figure 29, which contains 35 dispersion curves. The bandgaps for out of plane bands are shown in 4.1.3.

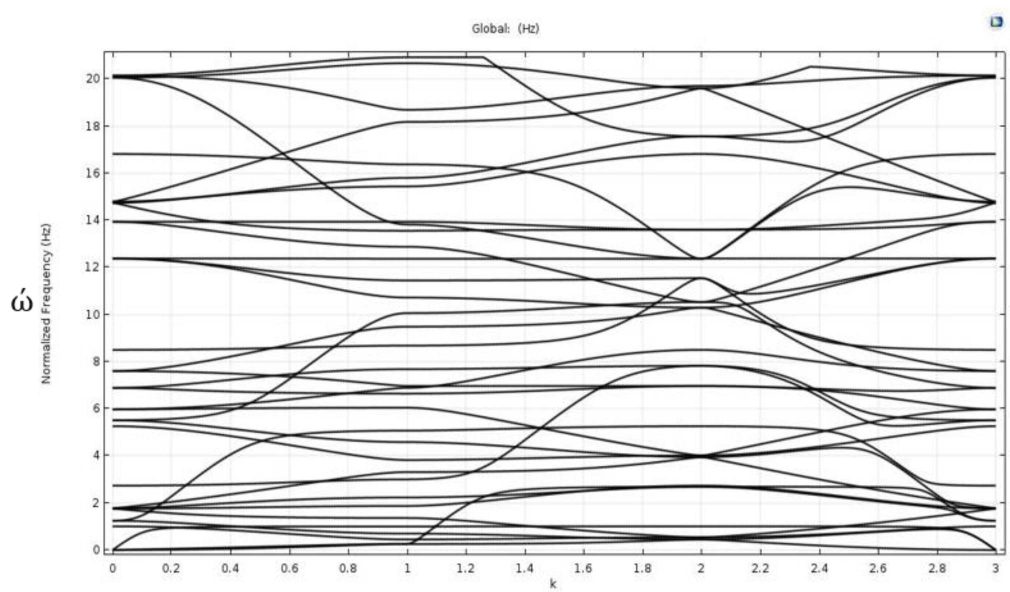

Figure 29. Square dispersion curves with in-plane and out of plane motions

4.1.3 in-plane & out of plane dispersion surfaces

Following a 25/25 grid to Figure the dispersion relation, brings about an increasingly comprehensible perspective on the band diagrams. The dispersion surfaces are appeared in Figure 30. for the in-plane square outcomes, while the out of plane surfaces have appeared in Figure.31. All the surfaces, including in-plane and out of the plane, are appeared in Figure 32. The blue part in each surface compares to the out of plane information, and the yellow part shows the in-plane information.

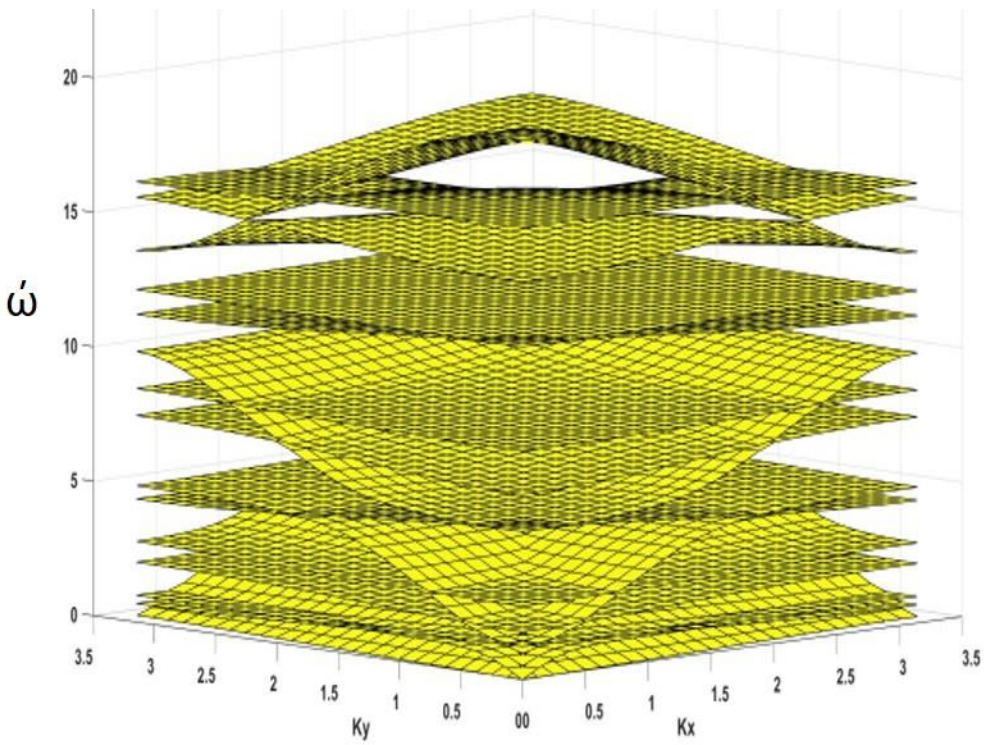

Figure 30. In-plane dispersion surfaces of the simple square lattice structure

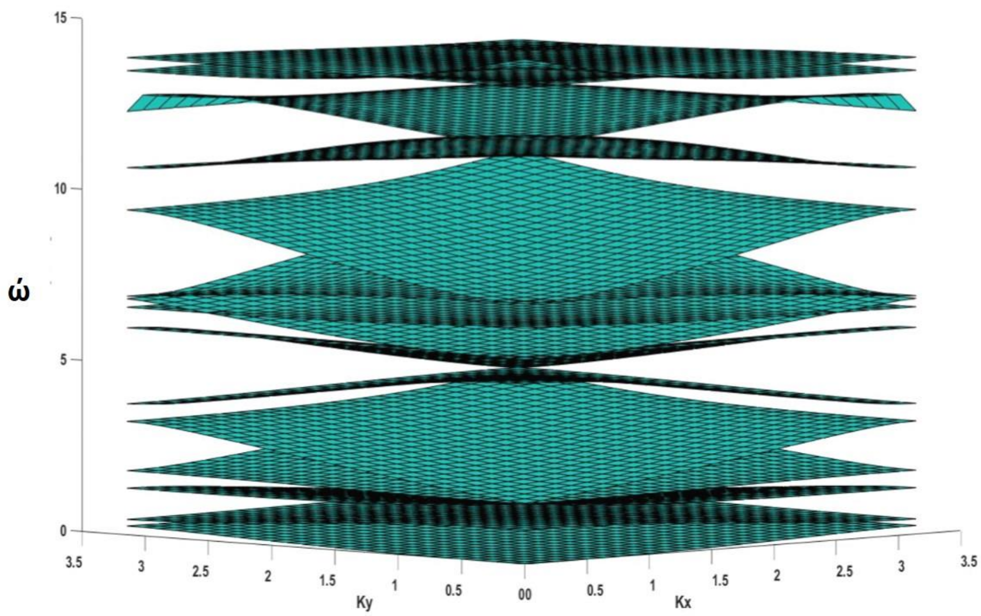

Figure 31. Out of plane dispersion surfaces of the simple square lattice structure

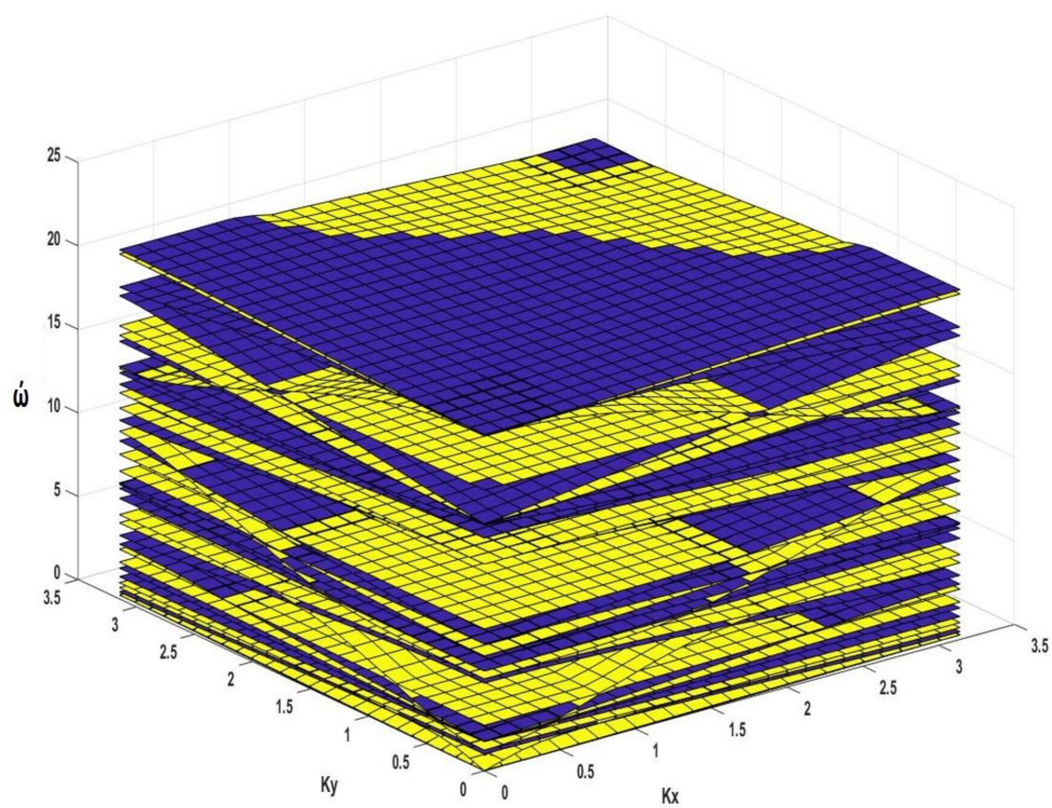

Figure 32. Dispersion surfaces comprising all the in-plane and out of plane surfaces

From Figure 32, we have the information of all the in-plane and out of plane surfaces from which we determine the information related to each surface independently and create them. The way towards making another surface by separating the data has appeared in section3. A detailed analysis of this will be shown in the next segment.

4.1.4 Polar group velocity plots for the square lattice

The polar plots shown in this section are from 0° to 90° since all the structures we consider are in symmetry with the first quadrant, we choose to show the group velocity direction and magnitude in that range.

All the data identified with the in-plane wave motions are presently exhibited as a polar plot. Figure 33. is the polar plot demonstrating the group velocity magnitude and the direction for all the in-plane surfaces in a simple square lattice structure. All the data identified with the bandgaps present, range of frequencies are talked about in the past areas by a sharp perception of the dispersion curves and the dispersion surfaces. All that study with additional information about the directivity from which we become acquainted with the course of the wave propagation at a specific frequency is displayed through Figure 33. From this, we will have the option to see the course of each frequency going inside the structure. Aside from this, we derive the data identified with the wave beaming. The significant deduction is about the speed of the waves going at every frequency and the direction of its propagation. We can watch the spots where there is no wave propagation occurring and where the speed is extremely high and exceptionally low.

Coming to this particular structure, we see that there are no complete bandgaps, which demonstrate the investigation produced using the dispersion relations in a progressively successful manner. All the pieces of data identified with the wave beaming and incomplete bandgaps, including the directivity in this structure, is talked in section 5.

Figure 34. shows the group velocity polar plot for the out of plane wave motions in the basic square lattice structure. Like the in-plane wave motions, there are no bandgaps for the out of plane wave motions in this structure. Since the structure is in symmetry, we see that the velocity maps underneath 45° reflect from 45° to 90°. Although we do not have any total bandgaps, despite everything, we do know a lot of partial bandgaps in the k_x and k_y headings. These things are talked about later.

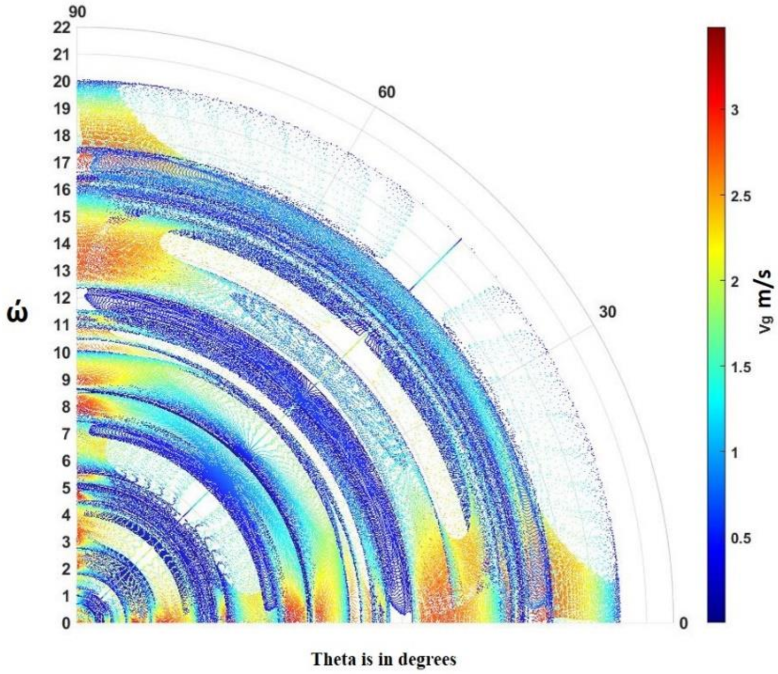

Figure 33. Polar plot indicating the magnitude and the direction of group velocity for the in-plane wave motions in a simple square lattice structure

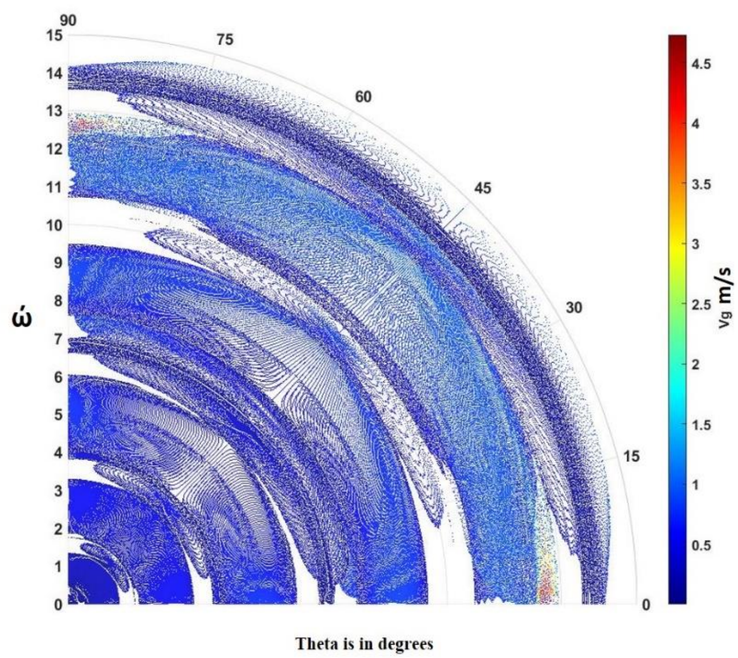

Figure 34. Polar plot indicating the magnitude and the direction of group velocity for the out of plane wave motions in a simple square lattice structure

4.2 Results & discussion - Simple square lattice structure.

A simple square lattice structure has no hierarchy. It does not consist of any bandgaps in it for both the in-plane and the out of the plane wave motions. This is observed in the study made by the dispersion curves and surfaces and through the group velocity polar plots. A detailed explanation about the complete and partial bandgaps for the in-plane and the out of the plane wave motions and the wave beaming characteristics are given in the following segments.

By looking at the group velocity polar plots, we see no locations where the wave cannot propagate inside the structure. So in this structure, under the first 15 eigenfrequencies, waves can propagate at all the frequencies in all the directions.

4.2.1 Partial bandgaps.

Though we do not have any complete bandgaps in this structure for both in-plane and the out of plane wave motions, we see some partial bandgaps in the direction of k_x and k_y in some locations and along the 45° direction at other locations.

Coming to the in-plane directionality plot, we can observe a very minute partial bandgap between 11.54 Hz and 12.37 Hz along the k_x and the k_y directions. Directions along k_x and k_y from the directionality plot means that the gaps are along the 0° direction and the 90° direction. There are no other partial gaps present along with these directions in this case.

We can observe some partial gaps along the 45° direction at some places. A gap with the width 17.3 Hz – 20 Hz is seen along 40° to the 50° direction. This gap has a large width whereas less angular range. Similarly, tiny gaps along the 45° direction are observed at frequencies like 12.41 Hz to 12.64 Hz and ώ = 13.81 Hz to ώ = 14.8 Hz, ώ = 5.5 Hz – 6.8 Hz, ώ = 1.2 Hz – 1.7 Hz and ώ = 2.9 – 3.9 Hz These are very minute but exist in the directionality plot where there is no chance for the in-plane wave propagation. All of these are shown in Figure 35.

When it comes to the out of plane wave motions in the square structure, the partial bandgaps are more compared to the in-plane wave motions. Since the structure is in symmetry in the first quadrant, all the gaps we observe are along k_x and the k_y Directions. In this case, the partial bandgaps are negligible along the 45° direction but, we see many gaps in between the frequency like ώ = 1 – 2, ώ = 3 – 4, ώ = 6 – 7, ώ = 7 – 8, ώ = 9 – 11 and ώ = 13- 14. All these are extended mostly from 0° to 20° or 75° to 90°. All of these can be observed in Figure 34.

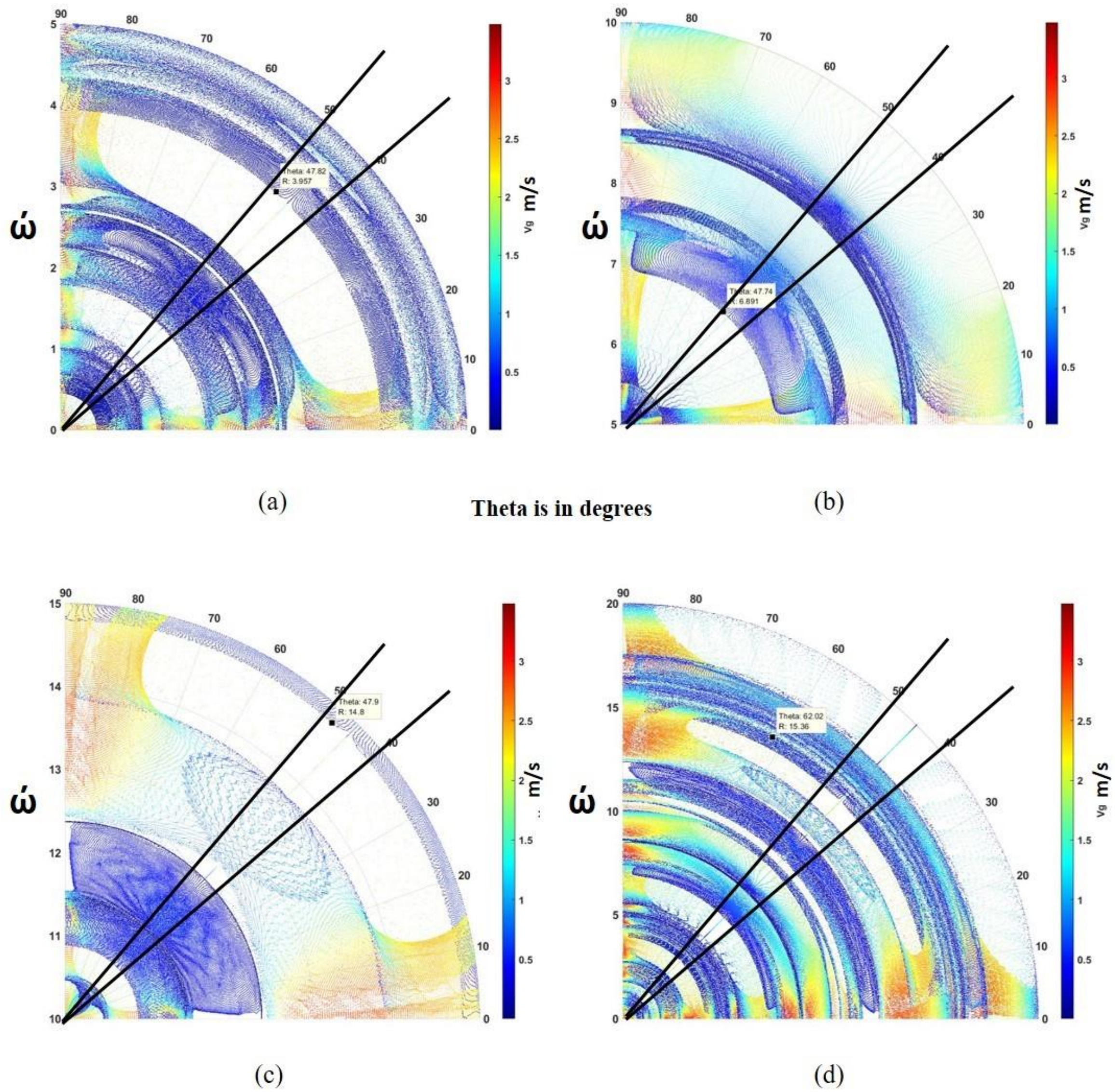

Figure 35 (a) Partial bandgaps indicated using two black lines under 0-5 Hz (b) Partial bandgaps indicated using two black lines under 5-10 Hz (c) Partial bandgaps indicated using two black lines under 10-15 Hz (d) Partial bandgaps under 15-20Hz

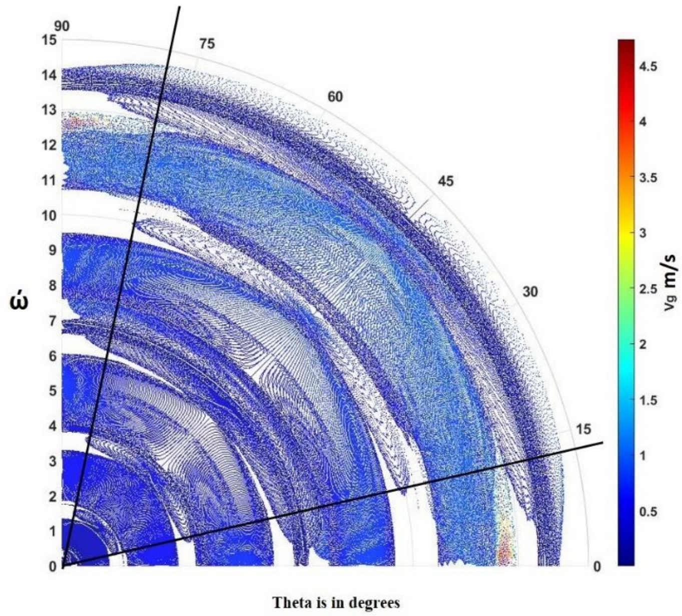

Figure 36. Partial bandgaps for the out of plane wave motions indicated using two black lines in the simple square structure.

4.2.2 Wave beaming effects.

Wave beaming, as discussed before, is the variation of the magnitude of the group velocity at every frequency level in a particular direction inside the structure. In this structure, we observe the effect of beaming for the in-plane wave movements along with the directions of k_x and k_y. The velocity of the wave propagating inside the structure is high along 0°– 15° or 85° to 90°. This indicates that the waves are propagating more and at high speed along the wave vectors. When the wave is traveling in the same direction as the wave vectors, the wave is at a high velocity when compared to the velocities in the middle part of the structure.

Speaking about the velocities of the out of plane wave movements, they are pretty consistent in the structure. Since we do not have any geometry of the structure in the z-direction, the velocities along the wave vector directions change in between ώ = 12 – 13 Almost at all the places inside the structure, the velocities are less than 2 m/s.

Another interesting fact about wave beaming is that we observe the location where the velocities are almost equal to 0 m/s. This means that they are close to creating a gap, and the wave propagation is nearly zero at those locations. From Figure 35, we see a position where the velocities are close to 0 m/s and can say that the structure at these frequencies vibrates very less.

Every single surface has its partial bandgaps. Overlapping all those surfaces gives us the group velocity plot for the entire structure. The nature of the wave propagation in every surface is different and have their own advantages.

4.3 The square in a square self-similar hierarchical lattice structure

A square in the square model is a self-similar hierarchical lattice structure. Since the order of hierarchy is increased when compared with a simple square structure, the band diagrams, surfaces would likewise be changed. Although it is similar to the base structure, they open up band gaps and also show a change in their directional nature. The frequencies in the square in a square lattice are normalized by 247.7 Hz

4.3.1 In-plane & out of plane dispersion surfaces

Similarly, a 25/25 grid is opted to Figure the dispersion relation. The dispersion surfaces are appeared in Figure 37. for the in-plane square outcomes, while the out of plane surfaces appear in Figure 38. All the surfaces, including in-plane and out of the plane, are appeared in Figure 39. The bandgaps can also be observed through the surfaces at the same frequency ranges as in the dispersion curves. We can see that the out of plane surfaces have more bandgaps when compared to the in-plane surfaces in this structure. More details about this will be mentioned in the next section.

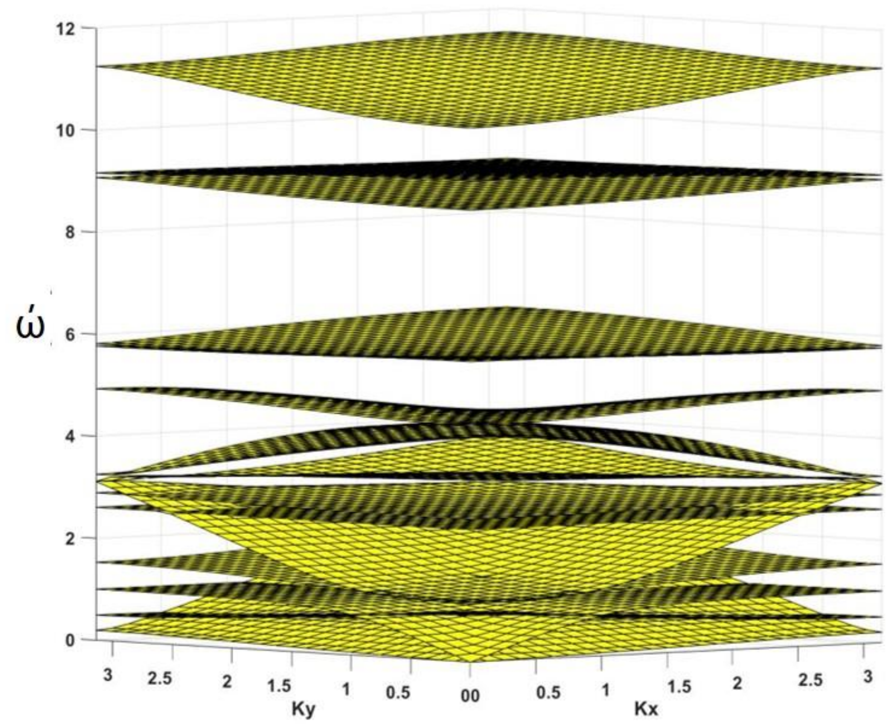

Figure 37. In-plane dispersion curves for the square in a square lattice structure.

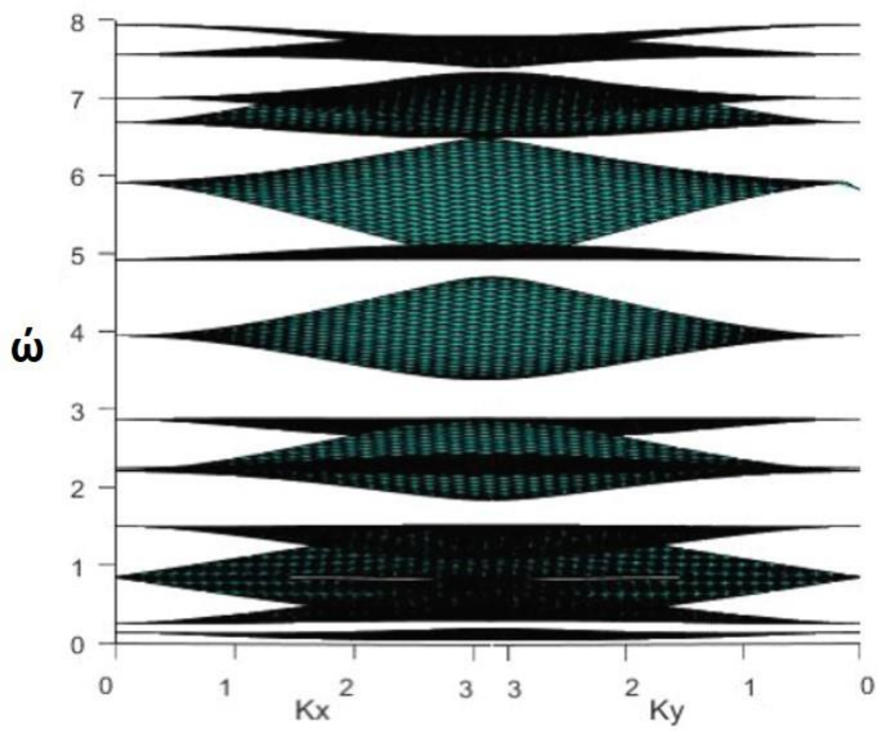

Figure 38. Out of plane dispersion surfaces for the square in a square lattice structure

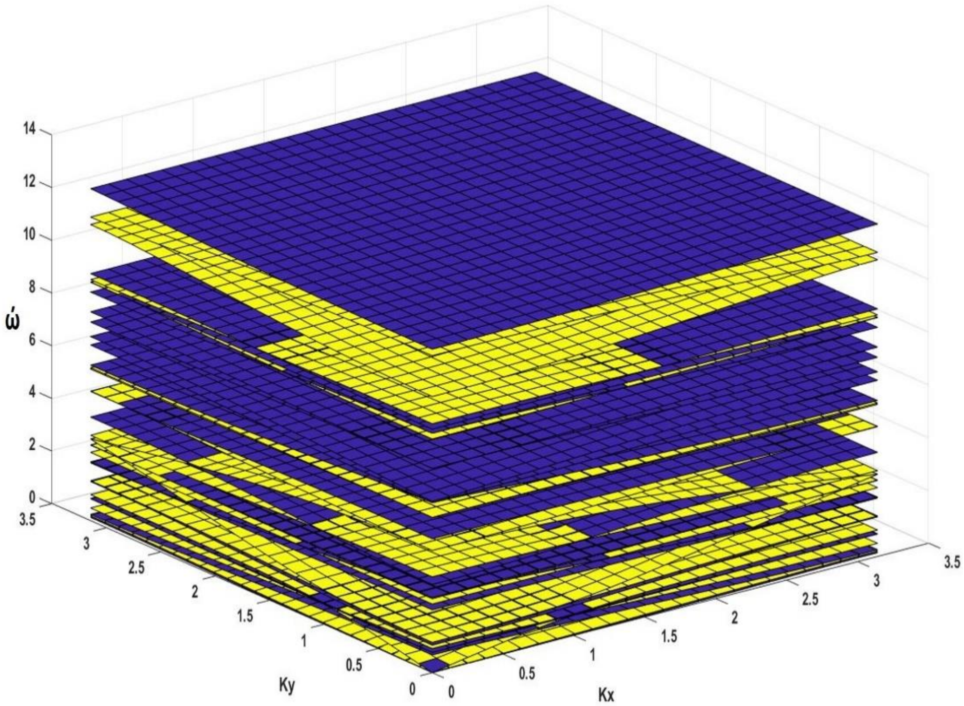

Figure 39. Dispersion surfaces of the square in a square lattice structure

4.3.2 Velocity plots for the square in square lattice structure.

Presently, we talk about the in-plane and out of plane wave motions in the square in a square hierarchical lattice structure through the polar group velocity plots. We realize that there are three complete bandgaps for the in-plane wave motions and five complete bandgaps for the out of plane wave motions from the examination we have done from the dispersion bends and dispersion surfaces.

Figure 40. shows the persistent velocity maps for all the in-plane surfaces in the square in a square structure. We see that the three bandgaps recorded before are noticeable plainly and all the more proficiently here through the velocity plots. The bandgaps are likewise at the same locations as in the dispersion relations. From this, we can unmistakably say that there is no wave spread or wave propagation in any of the directions inside the structure for the in-plane wave motions in those specific frequency zones.

Coming to the out of plane wave motions, Figure 41. shows the continuous velocity maps speaking to the magnitude and the direction of the group velocities for the out of the plane wave motions in the square in a square hierarchical lattice structure. As observed previously, we see all the five bandgaps referenced in Table 6.

The first bandgap has a minimum frequency range, and however, regardless, we can catch it productively through the polar velocity plot. The other four bandgaps are visible clearly under the frequency range achieved. We additionally observe various partial bandgaps in the k_x and $k_y$directions through the end, which is very noteworthy in this structure.

When compared with the simple square lattice structure, there is less wave beaming in the square in a square hierarchical lattice structure for the in-plane wave motions, and beaming appears very little changed for the out of plane wave motions. These will be examined in chapter 5.

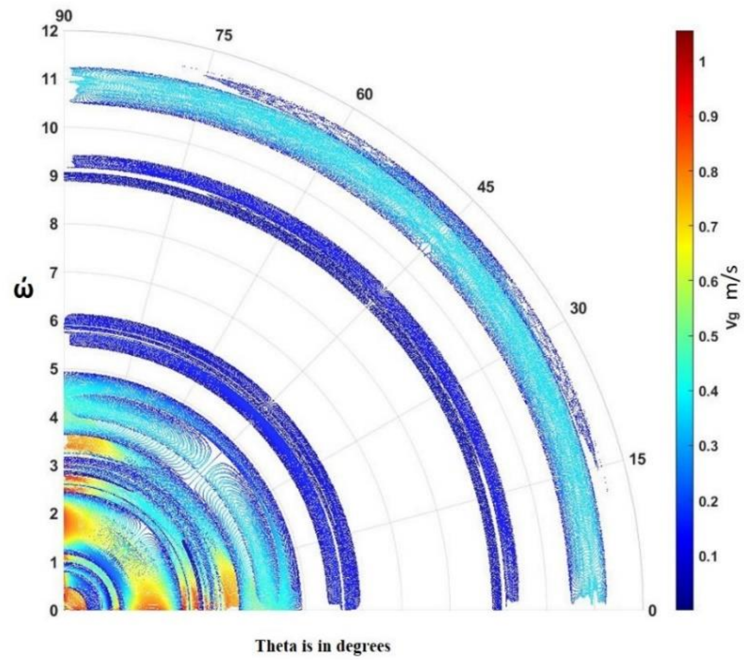

Figure 40. Polar plot indicating the magnitude and the direction of group velocity for the in-plane wave motions in the square in a square lattice structure

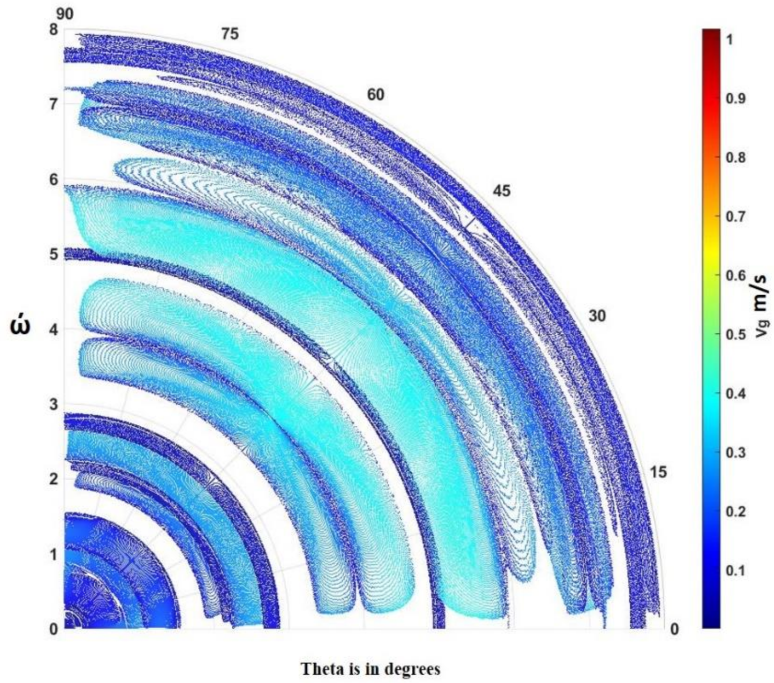

Figure 41. Polar plot indicating the magnitude and the direction of group velocity for the out of plane wave motions in the square in a square lattice structure

4.4 Results & discussion - Square in a square hierarchical lattice structure.

As a variation from the simple square lattice structure, introducing hierarchy increases the number of bandgaps at very low frequencies, and the velocity of the waves is reduced as the frequency keeps increasing. In this structure, we see that for the same number of surfaces considered, and the frequency range has dropped down to 12 Hz compared to the simple square lattice, which has its maximum frequency at 20 Hz for the in-plane wave motions as shown in Figure 40.

Similarly, in Figure 41, the frequency range is reduced to 8 Hz. It was around 15 Hz in the square lattice. From this, we understand that adding hierarchy decreases the frequency range of the structure, and we can achieve the bandgaps at low frequencies not only in case of the in-plane motions but also for the out of plane wave motions.

4.4.1 Partial bandgaps.

The partial bandgaps for the in-plane wave motions are decreased in this structure when compared to the square structure. There is a partial gap observed at ώ = 3 – 4. Almost every partial bandgap here is associated with a complete bandgap. Other partial gaps here are in between the frequencies ώ = 5.5 – 6.5, ώ = 8.5 – 9.5, and ώ = 10.5 – 11.5 as shown in Figure 42. There are minute gaps that can be observed in the 45°- direction as well.

For the out of plane wave motions, the partial bandgaps are close to 0° and 90°. The angular width of the gaps is very low for this structure. These are at ώ = 1.5 – 2, ώ = 3.5 – 4.5, ώ = 5 – 6 and ώ = 6 – 7.2. The partial gaps for the out of plane wave motions are shown in Figure 43.

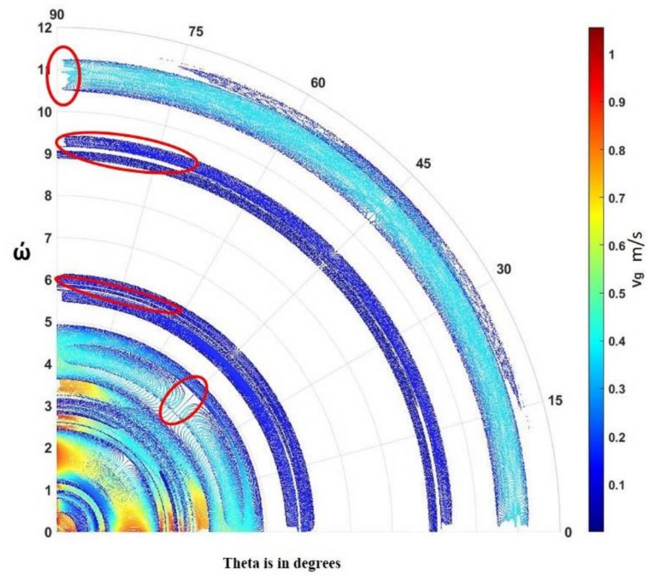

Figure 42. Partial bandgaps in the in of plane wave motions indicated using dark red circles in the square in a square structure.

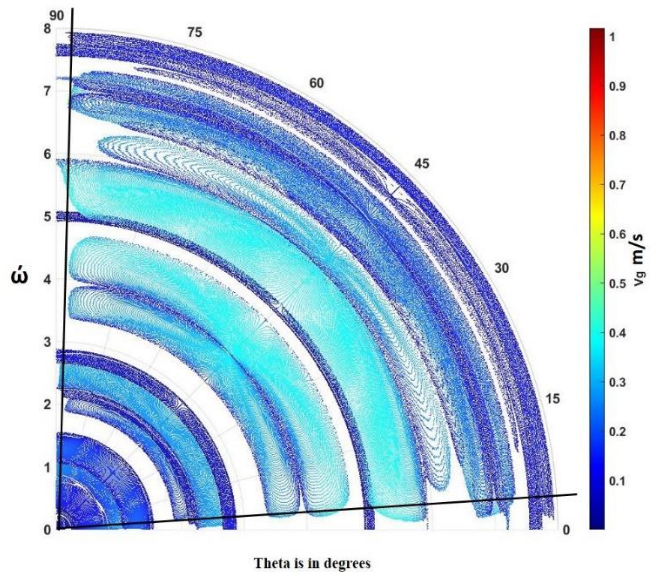

Figure 43. Partial bandgaps in the out of plane wave motions indicated using two black lines in the square in a square structure.

4.4.2 Wave beaming effects.

The velocity of the in-plane waves fluctuates more in the directions of the wave vector, similar to the square structure. However, it does not continue until the maximum frequency. From Figure 40, the magnitude of the group velocity reached the maximum values up to ώ = 4. After crossing that frequency, the magnitude of the velocities related to the in-plane wave motions decrease. From ώ = 5 – 10.4, the velocity of the waves is close to 0 m/s. This indicates that there will be no wave propagation in those frequency ranges since we have three bandgaps with larger width and velocities close to zero.

The variation of the group velocity of the waves for the out of plane wave movements in this structure is minimal. The maximum velocity of the out of plane waves is 0.4 m/s. The middle portion starting from ώ = 3 to ώ = 7 has the maximum magnitude. We can say that the wave propagation for the out of plane waves in this structure is very less.

4.5 The hexagon in a square lattice structure

A hexagon in a square lattice structure is a non-self-similar hierarchical lattice structure. Since we are considering to sweep the complete first quadrant of the unit cell, we can capture the symmetry of the structure. The frequencies in the hexagon in a square lattice are normalized by 382.87 Hz

4.5.1 In-plane & out of plane dispersion surfaces

The dispersion surfaces are showed up in Figure 44. for the in-plane square results, while the out of plane surfaces are showed up in Figure 45. All the surfaces, including in-plane and out of the plane, are showed up in Figure 46. The bandgaps can likewise be seen through the surfaces at a similar frequency as in the dispersion curves. We can see that the out of plane surfaces here have fewer bandgaps when contrasted with the in-plane surfaces in this structure.

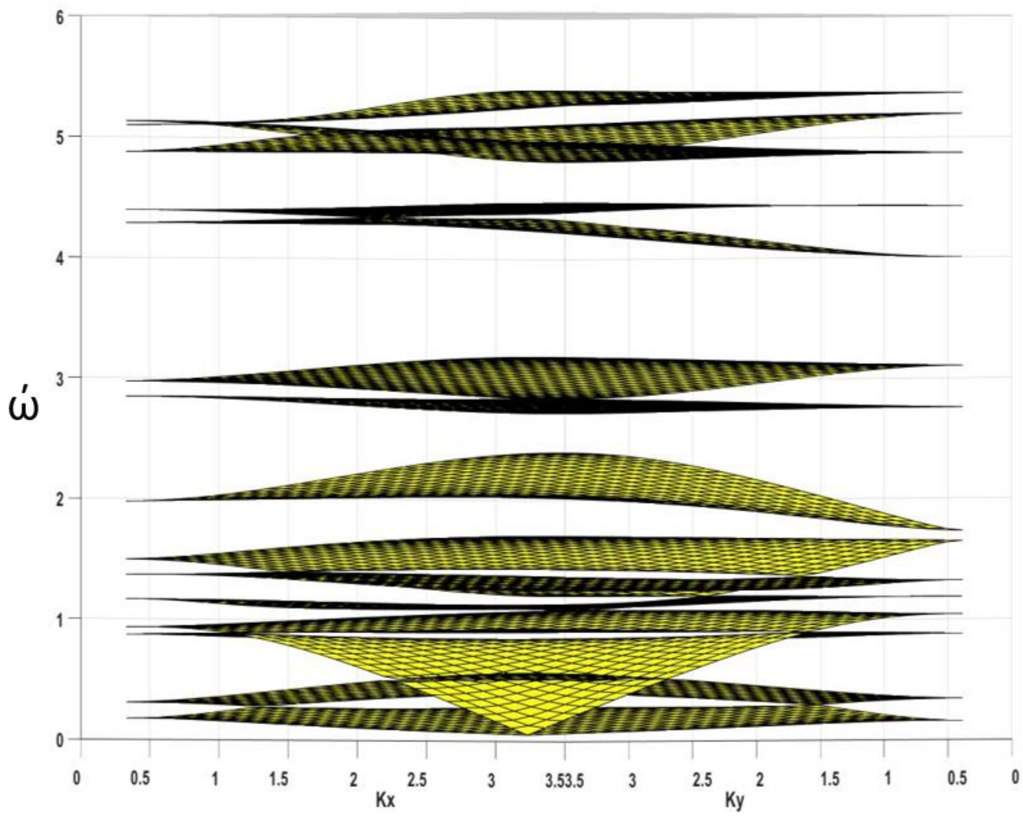

Figure 44. In-plane dispersion surfaces of the hexagon in a square lattice structure

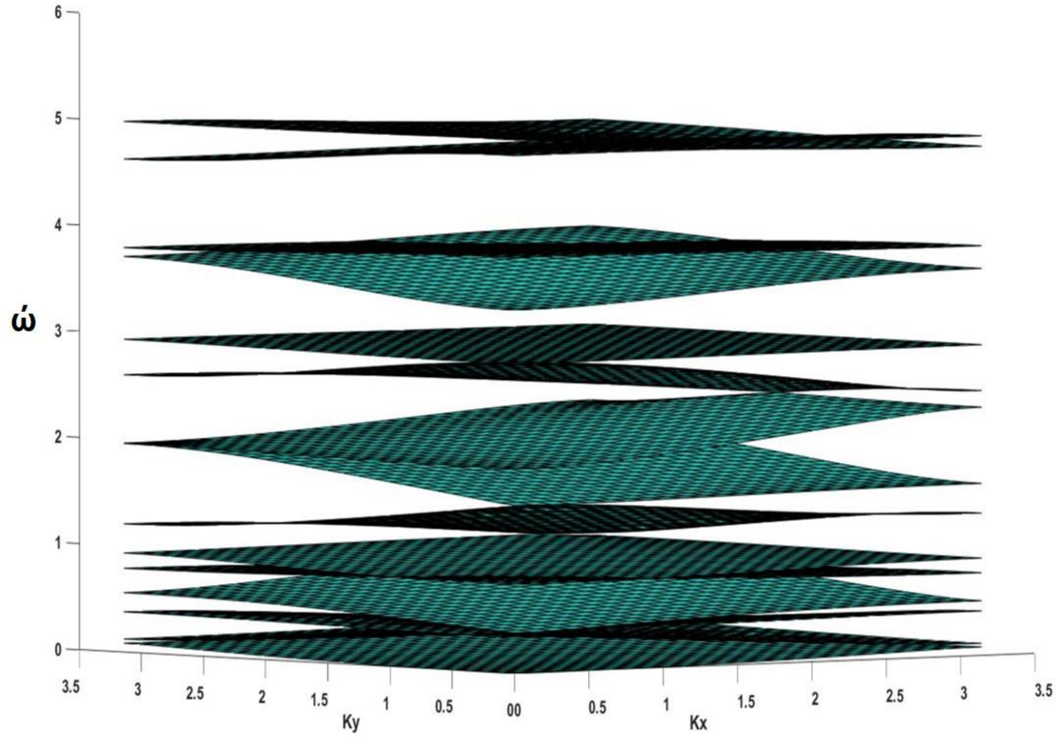

Figure 45. Out of plane dispersion surface for the hexagon in a square 3D lattice structure.

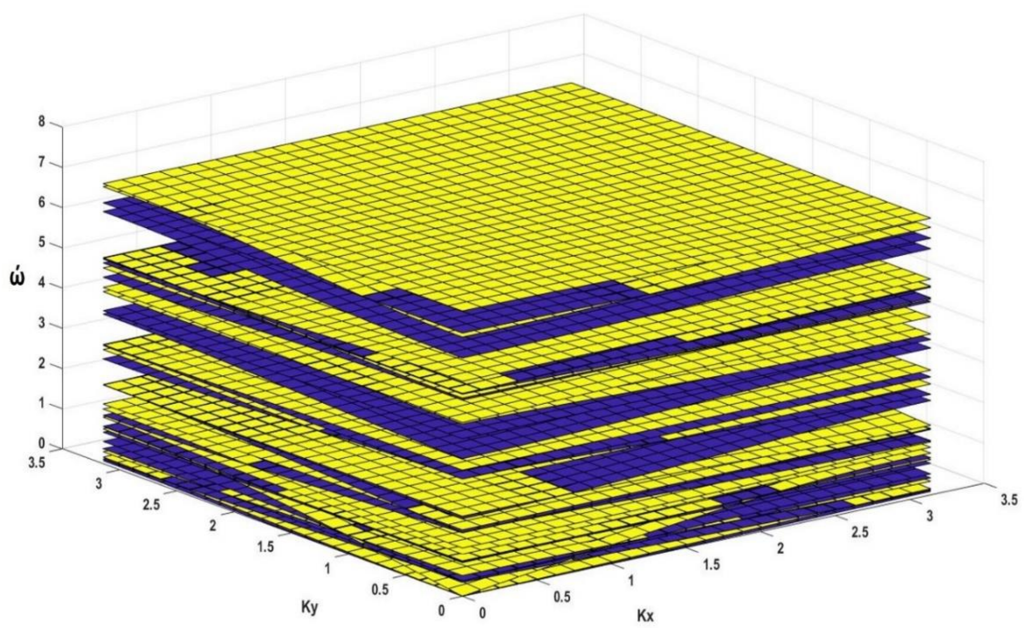

Figure 46: Dispersion surfaces for a hexagon in a square lattice structure for in-plane and out of plane wave motions.

4.5.2 Velocity plots for the hexagon in square lattice structure.

The hexagon in a square hierarchical lattice structure is diverse when contrasted with the other two structures. In this specific structure, we cannot watch the symmetry in the two halves of the first quadrant.

The in-plane wave motions in the hexagon in a square hierarchical lattice structure through a group velocity polar plot appear in Figure 47. Like the perceptions from dispersion surfaces, we see four complete bandgaps, which are at a similar frequency ranges.

The group velocity magnitude and direction for the out of plane wave movements in this structure are shown in Figure.48. From the velocity plots, we see that there are two bandgaps.

There are numerous fractional bandgaps in the group velocity plot for the out of plane wave movements, which is quite impressive when compared to the other structures.

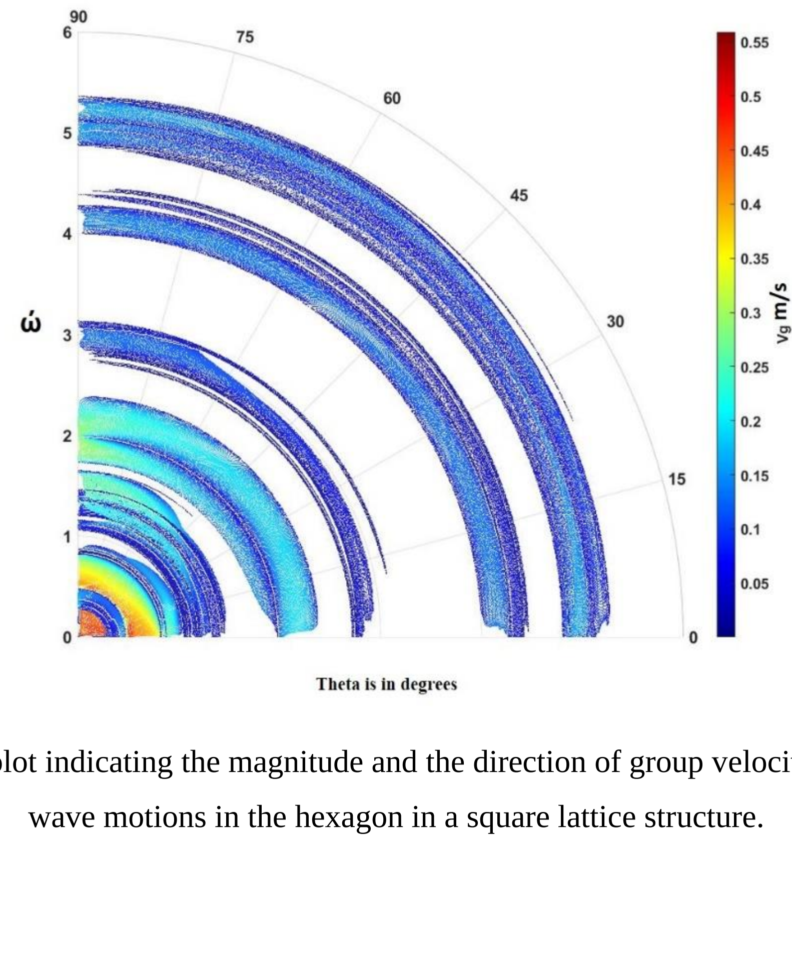

Figure 47. Polar plot indicating the magnitude and the direction of group velocity for the in-plane wave motions in the hexagon in a square lattice structure.

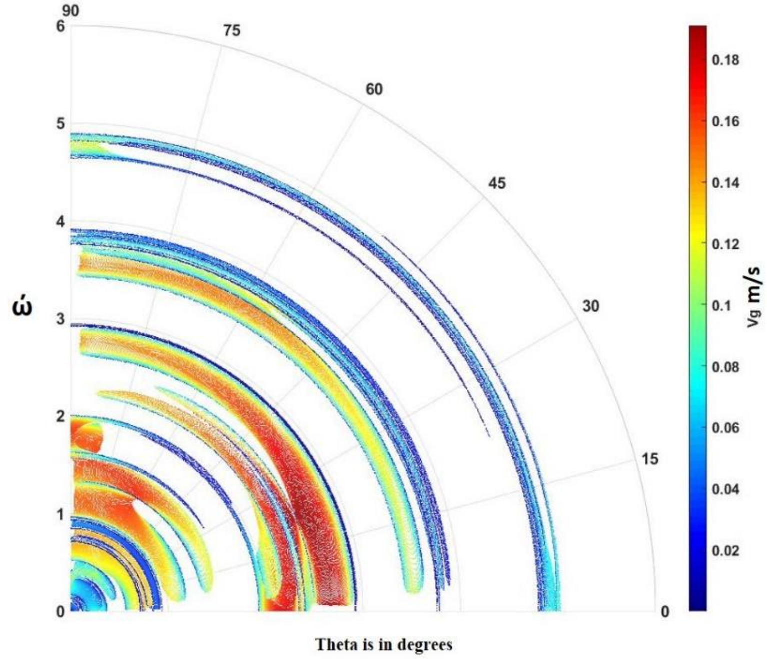

Figure 48. Polar plot indicating the magnitude and the direction of group velocity for the out of plane wave motions in the hexagon in a square lattice structure.

4.6 Results discussion - Hexagon in a square hierarchical lattice structure.

This is a non-self-similar hierarchical lattice structure. We do not see any symmetry in the first quadrant due to the geometry of the structure. From Figure 47, we can capture all the four bandgaps matching with the dispersion relation at the same frequency ranges. The in-plane bandgaps have increased when compared with the other two structures. For the out of plane wave motions, the complete bandgaps have decreased when compared with the other two structures. The frequency range for this structure is decreased to ώ = 6 for the out of plane waves and in-plane waves, which is less than the square and square in a square structure.

4.6.1 Partial bandgaps.

Partial bandgaps for the in-plane wave movements in this structure are observed to be less. There are two partial gaps at ώ = 1, which are broader in terms of the angular range and less wider in terms of the frequency range. It extends from 45° to 90° (W1 to W2 in Figure 49). The other partial bandgap observed is at ώ = 3. The angular extension is from 0° to 67° (Q1 to Q2 in Figure 49). These are shown clearly in Figure 49. There are very minute partial bandgaps present in this structure, which will be very clear when they are seen in that particular frequency range.

The out of plane wave motions in the hexagon in a square structure is very interesting in terms of the partial bandgaps. In this structure, the partial gaps have large angular width. They are denoted by Q1, Q2, and Q3, Q4 along the k_x direction and W1, W2, W3, W4 along the k_y direction. They are shown in Figure 50.

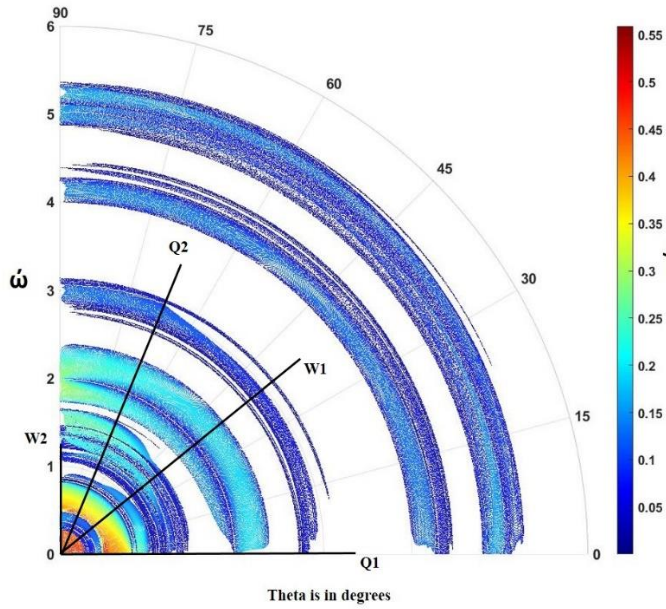

Figure 49. In-plane partial bandgaps for the hexagon in a square structure. The angular widths of the gaps are represented using the black lines. W1 - W2 indicates the first gap, and Q1 - Q2 represents the second.

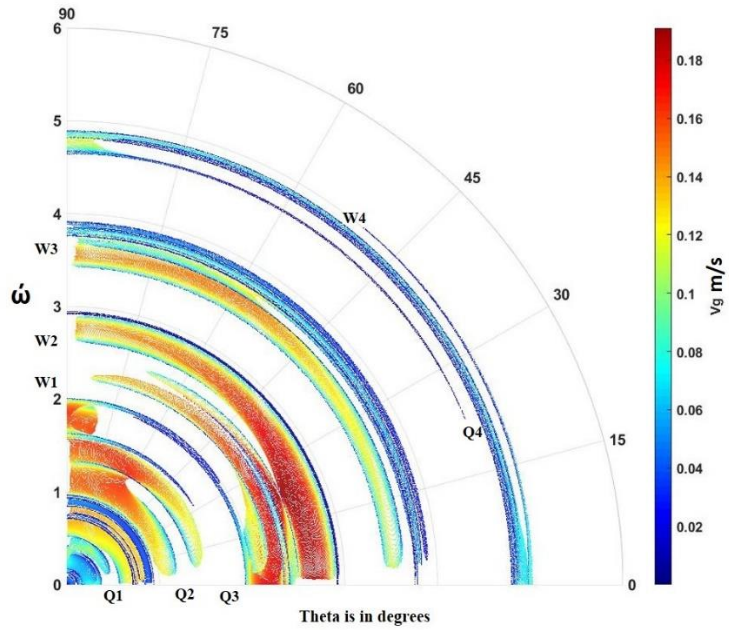

Figure 50. Out of plane partial bandgaps for the hexagon in a square structure represented by Q1, Q2, Q3, Q4 and W1, W2, W3, W4.

4.6.2 Wave beaming effects.

The magnitude of the group velocity of the waves decreases in this structure. The maximum value of the velocity is 0.55 m/s. The velocity starts at a higher level at lower frequencies and slowly starts to decrease. After ώ = 1, the velocity drops down to 0.25 m/s and lower, whereas the velocity is higher than 0.4 m/s under it for the in-plane wave motions.

When it comes to the out of plane wave movements, the velocity is very high in between ώ = 0.6 -3.6. The maximum velocity of 0.18 m/s is observed between ώ = 2 – 3 along 0° to 45°. After a certain level, as the frequency goes higher, we can see the magnitude of the group velocity decreases. Although we have many partial bandgaps in this structure for the out of plane wave motions, the wave propagates at a higher velocity in the range of it.

4.7 Variation of in-plane Bandgaps for the change in the type of structure

A more generalized study on the variation of the bandgaps for the in-plane wave motions in these structures is made in [59]. In any case, we consider showing the bandgaps which are under

15 curves for the square, square in a square, and hexagon in a square lattice structure. The bandgaps which happen due to the in-plane wave motions are shown in Table 3.

We see that there are no bandgaps in a simple square lattice. Be that as it may, when the hierarchy is implied in the simple square structure, the outcomes are unique. For a square in a square hierarchical lattice structure, there are three bandgaps which form because of the hierarchy. At the point when a non-self-similar hierarchical lattice structure like the hexagon in a square is chosen, the bandgaps happening due to the in-plane wave motions increment. The number of bandgaps in the hexagon in a square structure is 4.

Presently, we examine the frequency range of the bandgaps in the considered lattice structures. Having said about the number of bandgaps in each structure in Table 3, Table 4 shows the frequency scopes of each bandgap under 15 surfaces as considered for all the three structures chose in this study.

Table 3. Number of bandgaps in the considered structures

In-plane wave motions	
Number of bandgaps	Geometries
0	Simple square
3	Square in a square
4	Hexagon in a square

Table 4. Range of the bandgaps for the in-plane wave motions

The normalized frequency range of the bandgaps is in Hz for the in-plane wave motions			
Bandgap	Simple square	Square in a square	Hexagon in a square
1	--	4.93 - 5.46	1.58 - 1.67
2	--	6.14 - 8.86	2.31 - 2.62
3	--	9.44 - 10.47	3.02 - 3.86
4	--	--	4.29 - 4.65

As observed over, the maximum number of bandgaps we can get from these structures is 4. A simple square structure has no bandgaps, though the square in a square lattice structure has three bandgaps. The first is at ώ = 4.93 - 5.46 (Hz). The second bandgap is at ώ= 6.14 - 8.86 (Hz), and the third bandgap is at ώ= 9.44 - 10.47 (Hz). These are the frequency ranges of the three bandgaps in the square in a square lattice structure. Similarly, for the hexagon in a square lattice structure, we can see that there are four bandgaps formed under the first fifteen in-plane surfaces. The first bandgap formed is at ώ= 1.58 - 1.67 (Hz). The second bandgap can be seen at ώ= 2.31 - 2.62 (Hz). The third and the fourth bandgaps are at ώ= 3.02 - 3.86 (Hz) and ώ= 4.29 - 4.65 (Hz). Thus, these are the bandgaps shaped due to the in-plane wave motions in the considered hierarchical lattice structures.

All the perceptions are produced using Table 5. and Table 6. Figure 28. and Figure 30. showcase the bandgaps for a simple square lattice stricture. Figure 37. speaks about the bandgaps formed due to the in-plane wave motions for the square in a square lattice structure. Figure 44. shows the outcomes for the hexagon in a square hierarchical lattice structure.

All the bandgaps caused due to the in-plane wave motions, which are seen from the dispersion curves are again demonstrated all the more effectively utilizing the polar group velocity plots in the discussions segment. Each complete bandgap is shown with its width, and some partial bandgaps are additionally discussed in specific directions.

4.8 Variation of out of plane Bandgaps for the change in the type of the structure

Presently, we begin to examine the out of plane wave motions. In this portion, we talk about the variety of the bandgaps in the simple square, square in a square, and the hexagon in a square lattice structure. The results for the out of plane wave motions are distinctive when contrasted with the in-plane wave motions. Regardless, we consider demonstrating the bandgaps, which are under fifteen dispersion curves for the picked structures just like before. The number of bandgaps in each structure for the out of plane wave motions appears in Table 5.

Similar to the in-plane wave motions, there are no bandgaps for the out of plane wave motions in a simple square lattice structure. In any case, the square in a square hierarchical lattice structure has five bandgaps at various frequency ranges because of the impact of hierarchy. The bandgaps created for the in-plane wave motions are less than the bandgaps created for out of plane wave motions in the case of a square in a square lattice structure. While, for the hexagon in a square lattice structure, the number of bandgaps is diminished when contrasted with the bandgaps created for the in-plane wave motions. There are two bandgaps in the hexagon in a square structure.

Table 6. shows the frequency range of the bandgaps made under 15 surfaces for the out of plane wave motions in the chose structures.

Table 5. Number of bandgaps for the out of plane wave motion in the selected geometries

Out of plane wave motions	
Number of bandgaps	Geometries
0	Simple square
5	Square in a square
2	Hexagon in a square

Table 6. Range of the bandgaps for the out of the plane wave motions

The normalized frequency range of the bandgaps in Hz for out of plane wave motions			
Bandgap	Simple square	Square in a square	Hexagon in a square
1	--	0.22462 – 0.24902	2.946 – 3.421
2	--	1.55371- 1.875	3.916 – 4.644
3	--	2.877 – 3.345	--
4	--	4.737 – 4.919	--
5	--	7.359 – 7.426	--

After examining Table 6, we see that there are no bandgaps in a simple square lattice structure. In any case, the square in a square has five bandgaps. The first bandgap occurs at ώ = 0.22462 – 0.24902 (Hz). The second bandgap is at ώ= 1.55371-1.875 (Hz), and the third bandgap is at ώ= 2.877 – 3.345 (Hz). The fourth and the fifth bandgaps are at ώ= 4.737 – 4.919 (Hz) and ώ= 7.359 – 7.426 (Hz). Similarly, for the hexagon in a square lattice structure, we can see that there are two bandgaps formed under the initial fifteen out of plane surfaces. The first bandgap shaped is at ώ= 2.946 – 3.421 (Hz). The second bandgaps can be seen at ώ= 3.916 – 4.644 (Hz).

All these bandgaps for the out of plane wave motions can are hard to see from the dispersion curves since they are produced from the 3D geometries. These three-dimensional structures produce both in-plane and out of plane dispersion curves together. For this, we extricate the dispersion surfaces for the out of plane wave motions, which is likewise accomplished for the in-plane wave motions. All the bandgaps at the depicted frequency ranges can be found in Figure 30. for the simple square lattice structure. Figure 38. depicts the bandgaps for the square in a square hierarchical lattice structure. Figure 45. shows the two bandgaps framed for the out of plane wave motions through the dispersion surfaces in the hexagon in a square hierarchical lattice structure.

A better view at the bandgaps, partial bandgaps and the idea of directionality is accomplished through the group velocity polar plots appeared in the following segment.

4.9 Effects of hierarchy on group velocity magnitude and direction.

We have considered three different structures in this study: a simple lattice, a self-similar hierarchical lattice structure, and a non-self-similar hierarchical lattice structure. For the in-plane wave motions in all the structures, the change in the frequency ranges, and the group velocity magnitudes are shown in Table 7. displays the variation for the out of plane wave motions.

Table 7. Variation of the frequencies and group velocities for the three structures selected.

	Simple square		Square in a square		Hexagon in a square	
	In-plane	Out of plane	In-plane	Out of plane	In-plane	Out of plane
ώ (Hz)	0 - 20	0 - 15	0 - 12	0 - 8	0 – 5.5	0 - 5
Vg (m/s)	0 – 3.5	0 – 4.5	0 - 1	0 - 1	0 – 0.55	0 – 0.18

The frequency scope of the structures has diminished significantly, alongside the magnitude of the group velocity. From this, we comprehend that by changing the hierarchy, we can accomplish amazing outcomes from the structure at an exceptionally low-frequency level and build the number of bandgaps. The out of plane wave movements additionally shows some excellent results as we change the geometry of the structure. The changes in the out of the plane are similar to the in-plane wave movements. The number of bandgaps, when compared to the non-hierarchical structure, has increased at low frequencies.

Like the adjustment in the frequency scope of the structures, the group velocity size has likewise been decreased with the addition of hierarchy to the basic structure.

Considering the dispersion surfaces with both the in-plane and out of plane surfaces, we have made and isolated the surfaces utilizing the beta factor into fifteen in-plane surfaces and fifteen out of the plane surfaces. The methodology has been talked about in chapter 3. The surfaces made have additionally mirrored the outcomes from the dispersion bends and the group velocity polar plots, which makes us sure about the results accomplished in this work. We can likewise isolate the dispersion curves by utilizing the participation factors. However, to increase the exactness of the investigation, we have thought about a 25/25 grid, covering the whole first quadrant to get the outcomes for the structure in a thorough way instead of following a specific path to ponder the directionality of the structure. In any case, to make the necessary number of surfaces for a particular structure, the number of eigenfrequencies we determine ought to be at any rate double the number of surfaces we need to create or some of the time more than that.

5. CONCLUSION

This work investigates the characteristics of wave directionality in periodic lattice structures. The investigation is performed by joining the Floquet-Bloch theory of periodic structures with the FE method in Comsol multiphysics software. Two-dimensional (2D) Timoshenko beam elements are used to run the analysis. All the two-dimensional (2D) structures considered are designed in a three-dimensional medium (3D), and all the six degrees of freedom are considered to capture the in-plane and out of the plane wave motions. A thorough analysis is made to study the occurrence of bandgaps, partial bandgaps, and the effects of the geometry of the lattices in terms of wave directionality in three different kinds of lattice structure (a simple square lattice structure, the square in a square self-similar hierarchical lattice structure, and the hexagon in a square non-self-similar hierarchical lattice structure).

Participation factors are used to calculate the β-factor. A methodology using the β-factor is considered to derive the dispersion surfaces for a structure and extract the in-plane and out of plane surfaces from it. We have presented continuous frequency-dependent group velocity maps for the identification of full and partial bandgaps as well as wave beaming in the entire FBZ (First Brillouin Zone) in the simple square, the square in a square and the hexagon in square lattice structures. By isolating the in-plane and the out of plane modes, we have derived the continuous maps of group velocity magnitude vs. direction and frequency from studying the effects of structural symmetry and effects of hierarchy on the wave directionality. Unlike the dispersion relations, the group velocity plots show the wave propagation characteristics at every point in the IBZ (Irreducible Brillouin Zone) rather than a specific path in it. The thinplate spline interpolation method is used in this research work. The accuracy and the level of resolution can always be tailored by changing the type of interpolation and also by increasing the number of discrete points in the k-space based on which we calculate our dispersion surfaces and get our group velocity polar plots.

Complete stop-bands and partial bands in all the structures show that the hexagon in a square and the square in square structures have got both types of bands in its in-plane and also the out of plane wave modes. Whereas, the square lattice has no complete bandgaps in their in-plane modes. Structural symmetry plays a vital role in opening up the bands for the in-plane and the out of plane modes. For the in-plane wave modes, we can verify that no full bands are observed in the square lattice until the hierarchy is introduced in both the self-similar and non-self similar hierarchical lattice structures through the group velocity polar plots.

Even in the case of out of plane modes, we cannot generate any complete bandgaps until the hierarchy is introduced. Structural symmetries are different in the case of all the lattices we considered. On the bigger picture introducing hierarchy helps in generating bandgaps in the in-plane and out of plane modes, whereas the introduction of non-self similar hierarchy increases the angular width of the partial bands for both the in-plane and the out of plane modes.

The wave beaming effects are also altered with the change in the geometry of the structures. The in-plane wave motions have most of their beaming in 0° and 90° directions in the square lattice, whereas it reduces in the case of hierarchical lattice structures. Though there is a limited amount of beaming happening in the square, and square lattice structure, the out of plane modes show major beaming in the wave propagation for the hexagon in a square structure. The frequency range and the magnitude of the group velocity have also been reduced because of the hierarchical characteristics.

The present work focused on deriving the group velocity plots in understanding the concepts of wave directionality in the selected lattice structures. The future study can be done by analyzing the hollow lattices which have low-frequency deformation modes. Geometric parameters like the length, characteristic length, the diameter can be varied to generate more bands in dispersions. Carrying the study forward to undulated lattice structures would also be relevant research in opening more bands. Different structures with various geometric properties can be studied, and using them all to create a single finite structure can be used to tailor the directionality of the waves. Making this work gives us the ability to dictate the waves to travel in the required direction.

REFERENCES

REFERENCES

1. Itoh, T. *Periodic structures for microwave engineering*. in *MWE Microw. Workshop*. 2004.

2. Rizzi, S. and J. Doyle, *Spectral analysis of wave motion in plane solids with boundaries.* 1992.

3. Strutt, J.W. and B. Rayleigh, *The theory of sound*. 1945: Dover.

4. Langley, R.J.J.o.S. and Vibration, *On the modal density and energy flow characteristics of periodic structures.* 1994. **172**(4): p. 491-511.

5. Mead, D.J.J.o.s. and vibration, *Wave propagation in continuous periodic structures: research contributions from Southampton, 1964–1995.* 1996. **190**(3): p. 495-524.

6. Brillouin, L., *Wave propagation in periodic structures: electric filters and crystal lattices*. 2003: Courier Corporation.

7. Hussein, M.I., M.J. Leamy, and M.J.A.M.R. Ruzzene, *Dynamics of phononic materials and structures: Historical origins, recent progress, and future outlook.* 2014. **66**(4): p. 040802.

8. Sun, C.-T., J.D. Achenbach, and G.J.J.o.A.M. Herrmann, *Time-harmonic waves in a stratified medium propagating in the direction of the layering.* 1968. **35**(2): p. 408-411.

9. Nemat-Nasser, S.J.J.o.E., *General variational methods for waves in elastic composites.* 1972. **2**(2): p. 73-90.

10. Abrahamson, A., *The response of periodic structures to aero-acoustic pressures, with particular reference to aircraft skin-rib spar structures*. 1973, University of Southampton.

11. Mead, D.J.J.o.S. and Vibration, *A general theory of harmonic wave propagation in linear periodic systems with multiple coupling.* 1973. **27**(2): p. 235-260.

12. Ewins, D.J.J.o.M.E.S., *Vibration characteristics of bladed disc assemblies.* 1973. **15**(3): p. 165-186.

13. Griffin, J., T.J.J.o.V. Hoosac, Acoustics, Stress,, and R.i. Design, *Model development and statistical investigation of turbine blade mistuning.* 1984. **106**(2): p. 204-210.

14. Castanier, M.P., G. O´ ttarsson, and C. Pierre, *A reduced order modeling technique for mistuned bladed disks.* 1997.

REFERENCES

15. Deshpande, V. and N.J.I.J.o.I.E. Fleck, *High strain rate compressive behaviour of aluminium alloy foams.* 2000. **24**(3): p. 277-298.

16. Hazizan, M.A. and W.J.C.P.B.E. Cantwell, *The low velocity impact response of foam-based sandwich structures.* 2002. **33**(3): p. 193-204.

17. Fleck, N. and V.J.J.o.a.m. Deshpande, *The resistance of clamped sandwich beams to shock loading.* 2004. **71**(3): p. 386-401.

18. Talbot, J. and H.J.P.o.t.I.o.M.E. Hunt, Part C: Journal of Mechanical Engineering Science, *A computationally efficient piled-foundation model for studying the effects of ground-borne vibration on buildings.* 2003. **217**(9): p. 975-989.

19. Bao, J., Z. Shi, and H.J.J.o.E.M. Xiang, *Dynamic responses of a structure with periodic foundations.* 2011. **138**(7): p. 761-769.

20. Brun, M., et al., *Phononic band gap systems in structural mechanics: finite slender elastic structures and infinite periodic waveguides.* 2013. **135**(4): p. 041013.

21. Media, R.R., *Media.* 2020.

22. Sigalas, M. and E.N.J.S.s.c. Economou, *Band structure of elastic waves in two dimensional systems.* 1993. **86**(3): p. 141-143.

23. Ruzzene, M., et al., *Wave beaming effects in two-dimensional cellular structures.* 2003. **12**(3): p. 363.

24. Pennec, Y. and B. Djafari-Rouhani, *Fundamental properties of phononic crystal*, in *Phononic Crystals*. 2016, Springer. p. 23-50.

25. Liu, W., J.-W. Chen, and X.-Y.J.A.M.S. Su, *Local resonance phononic band gaps in modified two-dimensional lattice materials.* 2012. **28**(3): p. 659-669.

26. Kittel, C., *Elementary solid state physics: a short course*. 1962: Wiley.

27. Bacigalupo, A., M.J.I.J.o.S. Lepidi, and Structures, *Acoustic wave polarization and energy flow in periodic beam lattice materials.* 2018. **147**: p. 183-203.

28. Langley, R.S.J.J.o.s. and vibration, *The response of two-dimensional periodic structures to point harmonic forcing.* 1996. **197**(4): p. 447-469.

29. Trainiti, G., et al., *Wave propagation in undulated structural lattices.* 2016. **97**: p. 431-444.

REFERENCES

30. Gómez, S.E.R., *Wave propagation in a phase transforming cellular material*. 2016, Universidad EAFIT.

31. Rayleigh, L.J.T.L., Edinburgh,, D.P. Magazine, and J.o. Science, *XVII. On the maintenance of vibrations by forces of double frequency, and on the propagation of waves through a medium endowed with a periodic structure.* 1887. **24**(147): p. 145-159.

32. Cremer, L. and H.J.O.T.o.F.P.S. Leilich, Arch. Elektr. Uebertrag, *Zur theorie der biegekettenleiter.* 1953. **7**: p. 261-270.

33. Mead, D.J.J.J.o.S. and Vibration, *Free wave propagation in periodically supported, infinite beams.* 1970. **11**(2): p. 181-197.

34. Mead, D.J.J.J.o.E.f.I., *Vibration response and wave propagation in periodic structures.* 1971. **93**(3): p. 783-792.

35. Mead, D.J.J.o.S. and Vibration, *Wave propagation and natural modes in periodic systems: II. Multi-coupled systems, with and without damping.* 1975. **40**(1): p. 19-39.

36. Lin, Y.-K. and T.J.J.o.E.f.I. McDaniel, *Dynamics of beam-type periodic structures.* 1969. **91**(4): p. 1133-1141.

37. Faulkner, M., D.J.J.o.S. Hong, and Vibration, *Free vibrations of a mono-coupled periodic system.* 1985. **99**(1): p. 29-42.

38. Mead, D., A.J.J.o.S. Mallik, and Vibration, *An approximate method of predicting the response of periodically supported beams subjected to random convected loading.* 1976. **47**(4): p. 457-471.

39. Mead, D., S.J.J.o.S. Parthan, and Vibration, *Free wave propagation in two-dimensional periodic plates.* 1979. **64**(3): p. 325-348.

40. Mead, D., K.J.J.o.s. Pujara, and vibration, *Space-harmonic analysis of periodically supported beams: response to convected random loading.* 1971. **14**(4): p. 525-541.

41. Meza, L.R., et al., *Resilient 3D hierarchical architected metamaterials.* Proc Natl Acad Sci U S A, 2015. **112**(37): p. 11502-7.

42. Torquato, S., et al., *Effective mechanical and transport properties of cellular solids.* 1998. **40**(1): p. 71-82.

43. Gibson, L.J. and M.F. Ashby, *Cellular solids: structure and properties*. 1999: Cambridge university press.

REFERENCES

44. Shan, S., et al., *Multistable Architected Materials for Trapping Elastic Strain Energy.* Adv Mater, 2015. **27**(29): p. 4296-301.

45. Bayat, A. and S.J.J.o.A.M. Gaitanaros, *Wave directionality in three-dimensional periodic lattices.* 2018. **85**(1): p. 011004.

46. Foehr, A., et al., *Spiral-based phononic plates: From wave beaming to topological insulators.* 2018. **120**(20): p. 205501.

47. Nouh, M., et al., *Wave propagation in metamaterial plates with periodic local resonances.* 2015. **341**: p. 53-73.

48. Tie, B., B. Tian, and D.J.A.M.S. Aubry, *Theoretical and numerical investigation of HF elastic wave propagation in two-dimensional periodic beam lattices.* 2013. **29**(6): p. 783-798.

49. Tang, H.-W., W.-D. Chou, and L.-W.J.A.P.A. Chen, *Wave propagation in the polymer-filled star-shaped honeycomb periodic structure.* 2017. **123**(8): p. 523.

50. Spadoni, A., et al., *Phononic properties of hexagonal chiral lattices.* 2009. **46**(7): p. 435-450.

51. Wang, Y.-F., Y.-S. Wang, and C.J.J.o.P.D.A.P. Zhang, *Bandgaps and directional propagation of elastic waves in 2D square zigzag lattice structures.* 2014. **47**(48): p. 485102.

52. Casadei, F., J.J.I.J.o.S. Rimoli, and Structures, *Anisotropy-induced broadband stress wave steering in periodic lattices.* 2013. **50**(9): p. 1402-1414.

53. Bayat, A., F.J.S.M. Gordaninejad, and Structures, *Dynamic response of a tunable phononic crystal under applied mechanical and magnetic loadings.* 2015. **24**(6): p. 065027.

54. Langley, R., et al., *The response of two-dimensional periodic structures to harmonic point loading: a theoretical and experimental study of a beam grillage.* 1997. **207**(4): p. 521-535.

55. Zelhofer, A.J., D.M.J.I.J.o.S. Kochmann, and Structures, *On acoustic wave beaming in two-dimensional structural lattices.* 2017. **115**: p. 248-269.

56. Russell, D.A.J.P.S.G.P.i.A., *Acoustics and vibration animations.* 2001.

57. Britannica, E. *Wave velocity*. 2019; Available from: https://www.britannica.com/science/wave-velocity.

REFERENCES

58. Virta, K., *Numerics of Elastic and Acoustic Wave Motion*. 2016, Acta Universitatis Upsaliensis.

59. Muthu, I. and R. Nirmal, *Elastic wave propagation in self-similar and non-self-similar hierarchical lattice structures*. 2019, Wichita State University.

60. plates, B.a. *plates*. 2019; Available from: https://www.rocscience.com/help/rs3/pdf_files/theory/Beam-Plate.pdf.

61. *Force representations*. 2012; Available from: http://ae.msstate.edu/vlsm/forcesys/force_reps/unit_vector.htm.

62. *Phase and group velocity*. 2019; Available from: http://physics.gmu.edu/~dmaria/590%20Web%20Page/public_html/qm_topics/phase_vel/phase.html.

63. Zelhofer, A.J., *Computational Modeling of the Mechanics of Elastic Structural Lattices: Effects of Lattice Architecture and Hierarchy*. 2017, California Institute of Technology.

64. Mousanezhad, D., et al., *Honeycomb phononic crystals with self-similar hierarchy*. 2015. **92**(10): p. 104304.

65. Sun, Y., et al., *In-plane stiffness of the anisotropic multifunctional hierarchical honeycombs*. 2015. **131**: p. 616-624.

66. simSolid, A. *Modal participation factors*. 2016; Available from: https://blog.altair.com/simsolid-modal-participation factors/#:~:targetText=Modal%20participation%20factors%20%E2%80%93%20modal%20participation,contribution%20to%20the%20dynamic%20response.

67. Abaqus, *modal participation factors*. 2006.